CHAPTER 59

Surface and Interfacial Properties

Afshin Falsafi*, and Subu Mangipudi†, and Michael J. Owen‡

*3M Company, 3M Center, 260-2B-12, St. Paul, MN 55144
†Medtronic Corporation, 6800 Shingle Creek Parkway, Brooklyn Center, MN 55430
‡Dow Coming Corporation, Midland, MI, 48686-0994

59.1 INTRODUCTION

Quantitative surface and interfacial tension data for polymers are crucial to many aspects of the production and application of elastomers, plastics, textiles, films and coatings, foams, polymer blends, adhesives, and sealants. Although interface is the inclusive term for the region in space where two phases meet, if one of the phases is gaseous it is usually called a surface [1]. Thus we refer here to the surface tension of a polymer in air but to the interfacial tension between a polymer and a condensed phase such as water or another polymer.

A further nomenclature choice must be made between surface tension and surface free energy. The fundamental surface properties in capillarity can be thought of as the surface tension, i.e., force per unit length, and the surface free energy, i.e., free energy per unit area, which are numerically and dimensionally identical [2]. This is true for liquid surfaces that can assume an equilibrium shape but is not the case for solids where elastic forces complicate the issue and the surface state after measurement may be far from equilibrium. The surface tensions of liquids and solids are necessarily obtained in different manners. Liquid surface tensions are directly measured [3] and values are usually independent of the specific technique used, provided equilibrium is established, whereas solid surface tensions are generally derived from contact-angle measurements using semiempirical equations, yielding values dependent on the choice of liquids and equations.

The term *surface free energy* is more appropriate for a solid surface than surface tension, and we use it for the solid surface properties in this compilation with the exception of the earliest and most familiar contact-angle approach to polymer surface characterization, the Zisman critical surface tension of wetting [4]. The word *tension* is properly applied here as it refers to the liquid that just wets (zero contact angle) the solid. The contact-angle approaches only infer the surface free energy of solids; they do not measure it directly. To avoid confusion, note that some other polymer surface data compilations [5,6] use solid surface tension where we use surface free energy. We use the symbol γ in units of mN/m for liquid surface tension and critical surface tension of wetting and in units of mJ/m^2 for solid surface free energies. Note that the symbol σ is also used instead of γ, particularly in Europe.

Surface tension is the result of the imbalance of attractive forces between molecules at a surface. These may be very similar for a liquid and solid polymer of the same chemical constitution but, because they are derived differently, liquid surface tension and solid surface free energy need not have the same values for a particular polymer. For this reason separate tables of directly measured liquid

and contact angle-derived solid polymer surface properties are given. These two approaches account for most of the data available. There are a variety of other less exploited methods such as inverse gas chromatography that have been applied to polymers. The only one included here is that based on direct work of adhesion measurement by the Johnson, Kendall, and Roberts (JKR) equation [7].

59.2 LIQUID SURFACE TENSION

Liquid surface tensions γ_{LV} of selected homopolymers at 20 °C are given in Table 59.1. γ_{LV} is defined as the surface tension of the liquid in equilibrium with the saturated vapor pressure of the liquid. The table is not comprehensive. It is limited to the more important polymers, and where a datum

TABLE 59.1. *Liquid surface tension.*

Polymer	M_W	γ_{LV} at 20 °C (mN/m)	$-d\gamma/dT$[mN/(mK)]	References
Poly(oxyhexafluoropropylene)	∞	18.4 (25 °C)	0.059 (M_n − 7,000)	[17,10]
Poly[(heptadecafluorodecyl) methylsiloxane]	$M_n \sim$ 19,600	18.5 (25 °C)	—	[31]
Poly(dimethylsiloxane)	∞	21.3 (20 °C)	0.048 (10^6 cS)	[8,32]
Poly[methyl(trifluoropropyl)siloxane]	∞	24.4 (25 °C)	—	[31]
Poly(tetrafluoroethylene)	∞	25.6	0.053(M_n = 1,038)	[9]
Poly(oxyisobutylene)	M∼30,000	27.5	0.066	[6]
Poly(vinyl octanoate)	—	28.7	0.061	[33]
Polypropylene, atactic	Melt index ∼1,000	29.4	0.056	[32]
Paraffin wax	—	30.0 (20 °C)	∼0.06	[34]
Poly(1,2-butadiene)	$M_n \sim$ 1,000	30.4 (25 °C)	—	[35]
Poly(*t*-butyl methacrylate)	$M_v \sim$ 6,000	30.5	0.059	[23]
Poly(oxypropylene)	$M_n \sim$ 4,100	30.7 (25 °C)	0.073	[11]
Poly(*i*-butyl methacrylate)	$M_v \sim$ 35,000	30.9	0.060	[23]
Poly(chlorotrifluoroethylene)	$M_n \sim$ 1,280	30.9	0.067	[36]
Poly(vinyl hexadecanoate)	—	30.9	0.066	[33]
Poly(*n*-butyl methacrylate)	$M_v \sim$ 37,000	31.2	0.059	[37]
Poly(oxytetramethylene)	$M_n \sim$ 32,000	31.8	0.060	[38]
Poly(methoxyethylene)	$M_n \sim$ 46,500	31.8	0.075	[6]
Poly(*n*-butyl acrylate)	*M*∼32,000	33.7	0.070	[39]
Polyethylene, branched	$M_n \sim$ 7,000	34.3	0.060	[40]
Poly(isobutylene)	∞	35.6 (24 °C)	0.064 ($M_n \sim$ 2,700)	[8,41]
Polyethylene, linear	$M_w \sim$ 67,000	35.7	0.057	[41]
Poly(oxydecamethylene)	—	36.1	0.068	[42]
Poly(vinyl acetate)	$M_w \sim$ 120,000	36.5	0.066	[41]
Poly(2-methylstyrene)	$M_n \sim$ 3,000	38.7	0.058	[6]
Poly(oxydodecamethyleneoxyisophthaloyl)	—	40.0	0.070	[30]
Polystyrene	$M_v \sim$ 44,000	40.7	0.072	[37]
Poly(methyl acrylate)	$M_n \sim$ 25,000	41.0	0.070	[6]
Poly(methyl methacrylate)	$M_v \sim$ 3,000	41.1	0.076	[37]
Poly(epichlorohydrin)	$M_n \sim$ 1,500	43.2 (25 °C)	—	[43]
Polychloroprene	$M_v \sim$ 30,000	43.6	0.086	[23]
Poly(oxyethyleneoxyterephthaloyl)	$M_n \sim$ 16,000	44.5	0.064	[44]
Poly(oxyethylene)	∞	45.0 (24 °C)	0.076 (M_n − 6,000)	[45,32]
Poly(hexamethylene adipamide)	$M_n \sim$ 17,000	46.4	0.064	[44]
Poly(oxyisophthaloyloxypropylene)	—	49.3	0.083	[30]

Structural note regarding fluoropolymers in Tables 59.1 *and* 59.3: Rigorous application of nomenclature rules can lead to fluoropolymer names of excessive length for tabulations. There are few generally agreed abbreviations or acronyms for such polymers so rather than add to this problem we have dropped precise descriptions of substituent positions in the names in the tables. To avoid any confusion, the full names of these polymers are given below:
poly[(heptadecafluorodecyl)methylsiloxane] is poly[(1*H*, 1*H*, 2*H*, 2*H*-heptadecafluorodecyl)methylsiloxane], poly[methyl(trifluoropropyl)siloxane] is poly[methyl(1*H*, 1*H*, 2*H*, 2*H*-trifluoropropyl)siloxane], poly(heptadecafluorodecyloxymethylstyrene) is poly(1*H*, 1*H*, 2*H*, 2*H*-heptadecafluorodecyloxymethylstyrene), poly(pentadecafluorooctyl acrylate) is poly(1*H*, 1*H*-pentadecafluorooctyl acrylate), poly(pentadecafluorooctyl methacrylate) is poly(1*H*, 1*H*-pentadecafluorooctyl methacrylate), poly[heptadecafluorooctylsulfonamido(propyl)ethyl acrylate] is poly[2-(*N*-propyl-*N*-heptadecafluorooctylsulfonamido)ethyl acrylate], and poly[methyl(nonafluorohexyl)siloxane] is poly[methyl(1*H*, 1*H*, 2*H*, 2*H*-nonafluorohexyl)siloxane].

choice is possible only one reliable value has been chosen. The selection is guided by a preference for numerical rather than graphical data, studies of purified polymers, true equilibrium measurement techniques with a minimum of assumptions such as zero contact angle of the polymer with the material of construction of the measuring device, data on polymers of reported molecular weight, and original citations rather than subsequent compilations. Surprisingly some of the often quoted key values are in rather obscure sources. On occasion, for sufficiently important polymers, each of these preferences has been compromised in the preparation of Table 59.1 and the other tables.

The molecular-weight criterion is important since polymer liquid surface tension is a function of molecular weight. This is a density and end-group effect and is most apparent at low molecular weight. For this reason, either the highest-molecular-weight study is selected, in which case the actual molecular weight is given (MW column), or, if sufficient data are available, an extrapolated value to infinite molecular weight is given. This is shown in the MW column of Table 59.1 as ∞. All but one of these extrapolated selections use the LeGrand and Gaines equation [8]

$$\gamma_{LV} = \gamma_{\infty} - \boldsymbol{K}/\boldsymbol{M}_n^{2/3}, \tag{59.1}$$

where γ_{LV} is the surface tension at number average molecular weight M_n and K is a constant. The exception in Table 59.1 is the polytetrafluoroethylene γ_{∞} value which comes from extrapolation of γ_{LV}^{-1} vs n^{-1}, where n is the number of carbon atoms in the chain [9]. Wu [5] has given another alternative to Eq. (59.1). Equation (59.1) is used because most of the available data are presented in this manner. Sauer and Dee [10] have shown that theoretical predictions follow the $M_n^{-2/3}$ dependence for lower molecular weights and the M_n^{-1} dependence for high molecular weight. The difference between the surface tension of a polymer at $M_n \sim$ 3,000 and γ_{∞} is usually less than 1 mN/m.

If the polymer is a liquid at room temperature, the γ_{LV} at 20 °C column of Table 59.1 contains the actual data available nearest to 20 °C (the precise temperature of measurement is shown in parentheses). Other figures in this column are from extrapolation from higher temperature studies of polymer melts. The surface tension should change discontinuously at the crystal–melt transition and continuously at the glass transition with discontinuous $d\gamma/dT$, where T is the temperature in degrees Centigrade. Wu [5] has shown that extrapolation is usually adequate as semicrystalline polymers generally have amorphous surface when prepared by cooling from the melt, and the effect of glass transition temperature is small.

$d\gamma/dT$ data are not available at infinite molecular weight. Thus the highest-molecular-weight studies have been chosen in these instances and the molecular weight given in parentheses. When it is a separate study to the γ_{LV} at 20 °C data, a second citation is given in the reference column. Surface tensions of polymers vary linearly with temperature with $-d\gamma/dT$ typically being from 0.05 to 0.08; increasing γ_{LV} weakly correlates with larger values of $-d\gamma/dT$. This is somewhat less than the temperature coefficient for nonpolymeric liquids and is attributed to conformational restrictions of long-chain molecules, $-d_{\gamma}/dT$ being the surface entropy [5].

Table 59.1 is arranged, like all the tables in this compilation, in order of increasing surface tension so the familiar effect of polar constituent groups raising the surface tension is readily apparent. Most polymer chemists are familiar with Zisman's critical surface tension of the wetting [4] constituent effect (see Table 59.3) where the order of increasing surface tension is

$$CF_3 \rightarrow CF_2 \rightarrow CH_3 \rightarrow CH_2$$

A surprising aspect of Table 59.1 is the higher γ_{LV} at 20 °C (∞) value for CF_2 (polytetrafluoroethylene) than CH_3 (in the polydimethylsiloxane case).

No copolymer data are included in these tables. Random copolymers sometimes follow simple mixing expectations, e.g., random copolymers of ethylene oxide and propylene oxide show a linear dependence of liquid surface tension with mole fraction of propylene oxide over most of the composition range [11], but there are many deviations from this behavior [12]. This is probably due to development of significant sequence lengths of the lower-surface-tension component as block polymers can show marked preferential adsorption of the lower-surface-tension block [11,13].

No data on solutions are included either. Although there is considerable information in the literature on certain polymers, it is dependent on the particular choice of solvent and not amenable to systematic tabulation. The same is true of the wealth of adsorption from solution onto solids and spread film Langmuir trough data. Equations are available for calculating the surface tension of simple liquid mixtures that could be applied to polymers [14] and for calculating polymer solvent solution [15] surface tensions.

59.3 INTERFACIAL TENSION

Selected values of the interfacial tension at 20 °C between homopolymers γ_{12} are given in Table 59.2. Since these are studies of liquid polymers the table is constructed in a similar manner to Table 59.1 inasmuch as γ_{12} at 20 °C is extrapolated from higher-temperature studies except when an actual temperature is given in parentheses. Table 59.2 does not contain molecular-weight information. There are insufficient data available to make any predictions at infinite molecular weight. In large part these interfacial tension values are derived from the same materials that were used to obtain the temperature coefficient data in Table 59.1 and in these cases molecular-weight information can be obtained from that table.

TABLE 59.2. *Interfacial tension.*

Polymer pair	γ_{12} at 20 °C (mN/m)	$-d\gamma/dT$ [mN/(m K)]	References
Polychloroprene/polystyrene	0.5 (140 °C)	—	[23]
Polychloroprene/poly(*n*-butyl methacrylate)	1.6 (140 °C)	—	[23]
Poly(methyl methacrylate)/poly(*t*-butyl methacrylate)	3.0	0.005	[23]
Poly(methyl methacrylate)/polystyrene	3.2	0.013	[37]
Poly(dimethylsiloxane)/polypropylene	3.2	0.002	[6]
Poly(methyl methacrylate)/poly(*n*-butyl methacrylate)	3.4	0.012	[37]
Poly(dimethylsiloxane)/poly(*t*-butyl methacrylate)	3.6	0.003	[23]
Polybutadiene/poly(dimethylsiloxane)	4.0	0.009	[46]
Poly(methyl acrylate)/poly(*n*-butyl acrylate)	4.0	0.008	[6]
Poly(dimethylsiloxane)/poly(isobutylene)	4.0	0.016	[47]
Poly(*n*-butyl methacrylate)/poly(vinyl acetate)	4.2	0.011	[37]
Poly(dimethylsiloxane)/poly(*n*-butyl methacrylate)	4.2	0.004	[23]
Polystyrene/poly(vinyl acetate)	4.2	0.004	[23]
Polyethylene/polystyrene	4.4 (200 °C)	—	[48]
Poly(oxyethylene)/poly(oxtetramethylene)	4.5	0. 005	[38]
Polychloroprene/polyethylene, branched	4.6	0.008	[23]
Polyethylene, linear/poly(*n*-butyl acrylate)	5.0	0.014	[6]
Polyethylene, branched/poly(oxytetramethylene)	5.0	0.007	[38]
Poly(dimethylsiloxane)/polyethylene, branched	5.3	0.002	[38]
Poly(oxytetramethylene)/poly(vinyl acetate)	5.5	0.008	[38]
Polyethylene, branched/poly(*i*-butyl methacrylate)	5.5	0.010	[23]
Polyethylene, branched/poly (oxydodecamethyleneoxyisophthaloyl)	5.9	0.011	[30]
Polyethylene, branched/poly(*t*-butyl methacrylate)	5.9	0.016	[23]
Poly(dimethylsiloxane)/polystyrene	6.1	~0	[6]
Poly(dimethylsiloxane)/poly(oxytetramethylene)	6.4	0.001	[23]
Poly(dimethylsiloxane)/polychloroprene	7.1	0.005	[23]
Polyethylene, linear/poly(*n*-butyl methacrylate)	7.1	0.015	[37]
Polyethylene, linear/polystyrene	8.3	0.020	[37]
Poly(dimentylsiloxane)/poly(vinyl acetate)	8.4	0.008	[23]
Poly(isobutylene)/poly(vinyl acetate)	9.9	0.020	[41]
Polyethylene, linear/poly(methyl acrylate)	10.6	0.018	[6]
Polyethylene/poly(caprolactam)	10.7 (250 °C)	—	[48]
Poly(dimethylsiloxane)/poly(oxyethylene)	10.9	0.008	[38]
Polyethylene, branched/poly(oxyethylene)	11.6	0.016	[38]
Polyethylene, linear/poly(methyl methacrylate)	11.9	0.018	[37]
Polyethylene, linear/poly(vinyl acetate)	14.5	0.027	[41]
Polyethylene, linear/poly(hexamethylene adipamide)	14.9	0.018	[6]
Polyethylene, branched/poly(oxyisophthaloyloxypropylene)	15.4	0.030	[30]

Two points stand out when Tables 59.1 and 59.2 are compared; the temperature coefficients for interfacial tension are lower than those for surface tension, and there is no correlation between the interfacial tension of a polymer pair and the difference in their surface tensions. The former effect arises because the variation with temperature is a density effect.

The smaller magnitude of $-d\gamma_{12}/dT$ is due to the fact that $d(\rho_1 - \rho_2)/dT$ is less than $d\rho_1/dT$ or $d\rho_2/dT$, where ρ_i is the density of phase i. The latter effect shows that the interface between polymers is not simple. Equality of γ_{12} with $\gamma_1 - \gamma_2$ is Antonow's rule [16], the oldest such relationship. Clearly, few polymer pairs obey the rule. More complex relationships of this type are discussed in the following section.

There are also a few reports of interfacial tension of polymers with simpler liquids. Water is the most important of these liquids, e.g., the interfacial tension between water and poly(oxyhexafluoropropylene) is 53.1 mN/m at 25°C (Krytox AX, 300 cS viscosity [17]) and between water and poly(dimethylsiloxane) is 42.7 mN/m at 24°C at ($M_n \sim 1{,}000$[18]). Interfacial tensions with liquids can also be calculated from the equations discussed in Section 59.4 [Eqs. (59.6), (59.7), or (59.8)]. For example, King *et al.* [19] have calculated using the harmonic mean equation [Eq. (59.8)] that the interfacial tension with water of poly

(methyl methacrylate) is 24 mN/m while that for poly (hydroxyethyl methacrylate) is 0.1 mN/m.

59.4 SOLID SURFACE PROPERTIES

Solid surface properties based on contact-angle data for selected homopolymers are shown in Tables 59.3 and 59.4. The γ_c column of Table 59.3 is the Zisman critical surface tension of wetting [4] obtained from the quasistatic, advancing contact angles θ of a series of liquids of surface tension γ_{LV} by the empirical equation:

$$\cos\theta = 1 - b(\gamma_{LV} - \gamma_c), \tag{59.2}$$

where b is a constant. For nonpolar polymers the *n*-alkanes are a preferred set of homologous liquids to use and such data are indicated by footnote indicator *a* in the γ_c column.

Young's equation for the contact of a liquid (L) with a solid (S) is

$$\gamma_{LV}\cos\theta = \gamma_{SV} - \gamma_{SL}, \tag{59.3}$$

where γ_{LV} and γ_{SV} are defined as being in equilibrium with the saturated vapor (V) pressure of the liquid. From Eqs. (59.2) and (59.3) it follows that

$$\gamma_c = \gamma_{SV} - \gamma_{SL} \tag{59.4}$$

and other approaches to obtaining solid surface free energy from contact-angle data are essentially ways to calculate the usually unknown interfacial tension γ_{SL} between the polymer solid and the test liquid. These equations are of the form

$$\gamma_{SL} = \gamma_{SV} + \gamma_{LV} - F, \tag{59.5}$$

where F is given in a variety of ways, including

$$F = 2\left(\gamma_{LV}^{d}\gamma_{SV}^{d}\right)^{1/2}, \tag{59.6}$$

$$F = 2\left(\gamma_{LV}^{d}\gamma_{SV}^{d}\right)^{1/2} + 2\left(\gamma_{LV}^{p}\gamma_{SV}^{p}\right)^{1/2}, \tag{59.7}$$

$$F = 4\left(\gamma_{LV}^{d}\gamma_{SV}^{d}\right)/\left(\gamma_{LV}^{d} + \gamma_{SV}^{d}\right) + 4\left(\gamma_{LV}^{p}\gamma_{SV}^{p}\right)/\left(\gamma_{LV}^{p} + \gamma_{SV}^{p}\right). \tag{59.8}$$

In these equations γ^d is the dispersion force component and γ^p the other polar force components of surface free energy ($\gamma = \gamma^d + \gamma^p$). Equation (59.6) was introduced by Good and Girifalco [20] and Fowkes [21], Eq. (59.7) was introduced by Owens and Wendt [22], and Eq. (59.8) was introduced by Wu [23]. Data in Table 59.3 are mostly derived via Eq. (59.7) using water and methylene iodide; exceptions are noted by footnotes. Actual contact-angle data are usually, but not always, available in the references cited. As water is the ubiquitous liquid and used in many studies, a column for such data is included in Table 59.3. Where possible only quasistatic advancing contact-angle values were chosen.

Table 59.3 is based primarily on the Zisman critical surface tension of wetting and Owens and Wendt approaches because most of the polymer data available is in these forms. The inadequacies of equations such as Eq. (59.7) have been known for a decade, and newer, more refined approaches are becoming established, notably these of van Oss and coworkers [24]. A more limited number of polymers have been examined in this way and the data (at 20 °C) are summarized in Table 59.4. γ^{LW} is the component of surface free energy due to the Lifshitz–van der Waals (LW) interactions that includes the London (dispersion, γ^d), Debye (induction), and Keesom (dipolar) forces. These are the forces that can correctly be treated by a simple geometric mean relationship such as Eq. (59.6). γ^{AB} is the component of surface free energy due to Lewis acid–base (AB) polar interactions. As with γ^d and γ^p the sum of γ^{LW} and γ^{AB} is the total solid surface free energy. γ^{AB} is obtained from

$$\gamma^{AB} = 2(\gamma^{+}\gamma^{-})^{1/2}, \tag{59.9}$$

where γ^+ stands for the electron-acceptor parameter and γ^- for the electron-donor parameter of the surface free energy.

One of the problems of simple geometric and other combining rules is that none accounts for the occurrence of a zero polar surface free energy component between quite polar solids or liquids. If γ^+ is zero, i.e., for a monopolar material, then so will be γ^{AB}, however, large the value of γ^-. Moreover, the interfacial free energy equation that follows from Eq. (59.9) is a double asymmetrical interaction that allows the possibility of a negative interfacial free energy in certain cases. No absolute values of γ^+ and γ^- are known; the values in Table 59.4 are based on assumed values for reference liquids such as water, but note that the values of γ^{AB} are based only on the polarity ratios of γ^+ and γ^- relative to the reference liquid values and these polarity ratios can be precisely established. Table 59.4 is constructed from Tables XIII-5 and XIII-8A in van Oss's book [24]. These contain other copolymer and biopolymer surface-free-energy data (van Oss uses the term *surface tension* rather than *surface free energy*).

59.5 DIRECTLY MEASURED SOLID SURFACE FREE ENERGY

Surface free energies can be obtained from direct work of adhesion measurements using the Johnson, Kendall, and Roberts (JKR) [7] approach. According to the JKR theory, the contact radius a between two elastic bodies of radii of curvature R_1 and R_2, Young's moduli of E_1 and E_2, and Poisson ratios of ν_1 and ν_2, under an applied load P is given by

$$a^3 = \frac{R}{K}\left[P + 3\pi WR + \sqrt{6\pi WRP + (3\pi WR)^2}\right], \tag{59.10}$$

TABLE 59.3. *Solid surface properties,* γ_c, γ^d, γ^p.

Polymer	γ_c (mN/m)	Reference	γ^d (mJ/m^2)	γ^p (mJ/m^2)	Reference	$\theta(H_2O)$ (deg)	Reference
Poly(heptadecafluorodecyl oxymethylstyrene)	6[a]	[49]	9[b]	—	[49]	—	
Poly(pentadecafluorooctyl acrylate)	10.4[a]	[50]	—	—		—	
Poly(pentadecafluorooctyl methacrylate)	10.6[a]	[51]	9.1	0.3	[22]	119	[51]
Poly[heptadecafluorooctyl sulfonamido(propyl) ethylacrylate]	11.1[a]	[51]	10.3	0.4	[52]	118	[51]
Poly(hexafluoropropylene)	16.2[a]	[53]	11.7	0.7	[52]	—	
Poly[methyl(nonafluorohexyl) siloxane]	16.3[a]	[54]	8.4	1.1	[54]	115	[54]
Poly(tetrafluoroethylene)	18.3[a]	[55]	18.6	0.5	[22]	108	[22]
Poly[methyl(trifluoro)siloxane]	21.4[a]	[56]	10.8	2.8	[56]	104	[56]
Poly(trifluoroethylene)	22	[57]	19.9	4.0	[22]	92	[57]
Paraffin wax	23	[22]	25.4	0	[22]	112	[58]
Poly(dimethylsiloxane)	24	[59]	21.7	1.1	[22]	101	[22]
Poly(vinylidene fluoride)	25	[57]	23.2	7.1	[22]	82	[57]
Poly(1,2-butadiene)	25	[60]	—	—		—	
Poly(isobutylene)	27	[60]	—	—		—	
Poly(vinyl butyral)	28	[60]	—	—		—	
Poly(vinyl fluoride)	28	[57]	31.3	5.4	[22]	80	[57]
Polypropylene	29	[61]	28.6	0.4	[35]	116	[35]
Poly(chlorotrifluoroethylene)	31	[62]	23.9	3.6	[23]	90	[62]
Polyisoprene, *cis*	31	[63]	—	—		106	[63]
Poly(oxypropylene)	32	[60]	—	—		—	
Poly(*n*-butyl methacrylate)	32	[64]	31.3	2.0	[23]	91	[23]
Polystyrene	32.8	[65]	41.4	0.6	[22]	91	[65]
Polyethylene, branched	33	[66]	32.0	1.1	[22]	94	[66]
Poly(undecanoamide)	33	[67]	—	—		89	[67]
Poly(epichlorohydrin)	35	[63]	—	—		87	[63]
Poly(vinyl alcohol)	37	[68]	—	—		—	
Poly(vinyl acetate)	37	[60]	—	—		—	
Polychloroprene	38	[63]	—	—		—	
Poly(vinyl chloride)	39	[57]	40.0	1.5	[22]	87	[57]
Cellulose acetate	39	[69]	—	—		65	[69]
Poly(methyl methacrylate)	39	[70]	35.9	4.3	[22]	80	[70]
Poly(vinylidene chloride)	40	[57]	42.0	3.0	[22]	80	[57]
Poly(oxyphenylene)	41	[60]	—	—		—	
Polycaprolactam	42	[64]	—	—		70	[64]
Poly(hexamethylene adipamide)	42.5	[65]	40.8	6.2	[22]	72	[22]
Poly(oxyethyleneoxyterephthaloyl)	43	[65]	43.2	4.1	[22]	76	[22]
Poly(ethylene oxide)	43	[60]	—	—		—	
Poly(acrylonitrile)	44	[60]	—	—		—	
Polyglycine	44	[71]	—	—		49	[71]
Cellulose, regenerated	44	[68]	—	—		—	
Poly(ether ketone ketone)	—		41.7	6.5	[35]	85	[35]
Poly(2-hydroxyethyl methacrylate)	52	[72]	34.1[c]	24.3[c]	[72]	—	
Poly(acrylamide)	52.3	[73]	—	—		—	
Urea–formaldehyde resin	61	[74]	—	—		—	

[a]Determined using *n*-alkane contact-angle test liquids.
[b]Determined by use of Eq. (59.6).
[c]Determined by use of Eq. (59.7) but using methylene iodide and glycerol (not water).

TABLE 59.4. *Solid surface properties* γ^{LW},γ^{AB}.

Polymer	γ^{LW} (mJ/m^2)	γ^{AB} (mJ/m^2)	γ^+ (mJ/m^2)	γ^- (mJ/m^2)	Reference
Poly(tetrafluoroethylene)	18.5	0	0	0	[75]
Poly(isobutylene)	25.0	0	0	0	[76]
Poly(propylene)	25.7	0	0	0	[76]
Polyethylene	33.0	0	0	0	[77]
Poly(hexamethylene adipamide)	36.4	1.3	0.02	21.6	[78]
Poly(methyl methacrylate)	41.4	0	0	12.2	[78]
Poly(oxytetramethylene)	41.4	2.6	0.06	27.6	[24]
Polystyrene	42	0	0	1.1	[24]
Poly(vinyl alcohol)	42	0	0	17–57	[79]
Poly(vinyl chloride)	43	0.75	0.04	3.5	[76]
Poly(vinyl pyrrolidone)	43.4	0	0	29.7	[24]
Cellulose	44.0	10.5	1.6	17.2	[24]
Cellulose nitrate	44.7	0.4	0.003	13.9	[80]
Cellulose acetate	44.9	7.7	0.8	18.5	[24]
Poly(oxyethylene)	45.9	0	0	58.5	[24]

where

$$\frac{1}{R} = \frac{1}{R_1} + \frac{1}{R_2}, \tag{59.11}$$

$$\frac{1}{K} = \frac{3}{4}\left[\frac{1-\nu_1^2}{E_1} + \frac{1-\nu_2^2}{E_2}\right] \tag{59.12}$$

and W is the *thermodynamic work of adhesion*. For two identical surfaces in contact:

$$W = 2\gamma \tag{59.13}$$

and, for two dissimilar surfaces in contact:

$$W = \gamma_1 + \gamma_2 - \gamma_{12} \tag{59.14}$$

γ_1,γ_2 are the surface energies of materials 1 and 2, and γ_{12} is the interfacial energy between 1 and 2.

Equation (59.10) may be rearranged as

$$W = \frac{\left(P - \frac{a^3 K}{R}\right)^2}{6\pi K a^3}. \tag{59.15}$$

When the surfaces are in contact due to the action of the attractive interfacial forces, a finite tensile load is required to separate the bodies from adhesive contact. This tensile load is called the ''pull-off'' force (P_s). According to the JKR theory, the pull-off force is related to the thermodynamic work of adhesion (W) and the radius of curvature (R).

$$P_s = \frac{3}{2}\pi W R. \tag{59.16}$$

γ_{JKR} values are presently not extensive in number but offer instructive comparisons with contact angle studies. This is done in Table 59.5. The references cited are to the JKR values, γ_{JKR}. Other data for the four polymers come from Tables 59.1 and 59.3. The poly(oxyethyleneoxyterephthaloyl) (PET) and polyethylene (PE) JKR studies of Tirrell and coworkers [25,26] are on samples biaxially stretched during sample preparation, so these surfaces should be semicrystalline in contrast to the amorphous surfaces used for most contact-angle studies. Despite this, their contact angle studies on the same samples used in the JKR studies gave values similar to other contact angle studies such as those listed in Table 59.3. This implies little difference between amorphous and semicrystalline surfaces in these two instances; another explanation is needed for the unexpectedly high JKR surface-free-energy values for poly(oxyethyleneoxyterephthaloyl).

Also included in Table 59.5 are data for various self-assembled silane monolayers formed on plasma-oxidized polydimethylsiloxane (PDMS) surfaces [27] that offer a measure of the effect of changing the outermost groups on a polymer surface. The γ^d_{SV} data come from Eq. (59.7) using water and methylene iodide, except for the perfluoromethyl surface for which the contact angle of perfluorodecalin was used. The comparative γ_c and γ_{LV} figures come from Shafrin and Zisman [28] and Wu [6], respectively. A more extensive compilation of γ_c and $\gamma^d{}_{SV}$ and $\gamma^p{}_{SV}$ for functional silane layers is available [29] but comparative γ_{JKR} data are currently lacking.

To understand the reasons for different predictions of different methods, Li *et al*. [83] measured the adhesion between a variety of polymers with well-controlled backbone chemistry These polymers include: poly(4-methyl 1-pentene) [TPX], poly(vinyl cyclohexane) [PVCH], polystyrene [PS], poly(methyl methacrylate) [PMMA], and poly(2-vinyl pyridine) [PVP], poly(4-*tert*-butyl styrene) [PtBS], poly(acrylonitrile) [PAN], poly(*p*-phenyl styrene) [PPPS], poly(vinyl benzyl chloride) [PVCB]. It may be noted that, among the polymers listed above, TPX and PVCH are purely dispersive in nature. PS is predominantly dispersive with some dipole-induced dipole interactions.

TABLE 59.5. *Surface free energy comparisons.*

Polymer or terminal surface functionality	$\gamma_{JKR}(mJ/m^2)$	Reference	$\gamma_C(mN/m)$	$\gamma_{LV}(mN/m)$	$\gamma^d{}_{SV}(mN/m)$
Poly(dimethylsiloxane) [PDMS]	22.6	[27]	24	21.3	22.8
Natural rubber (*cis* 1,4 polyisoprene)	35	[7]	31	—	—
Poly(oxyethyleneoxyterephthaloyl)	61.4	[25]	43	44.5	47.3
Polyethylene	33	[26]	32	34.3	32.0
Corona-treated polyethylene	52	[83,84]	34	—	—
Poly(4-methyl 1-pentene)	27	[83,84]	22	—	—
Poly(vinyl cyclohexane)	28	[83,84]	29	—	—
PS polystyrene	44	[83,84]	30	—	—
Poly(2-vinyl pyridine)	63	[83,84]	50	—	—
Poly(methyl methacrylate)	53	[83,84]	40	—	—
$-CF_3$	16.0	[27]	6	15	15.0
$-CH_3$	20.8	[27]	22	30	20.6
$-OCH_3$	26.8	[27]	—	—	30.8
$-CO_2CH_3$	33.0	[27]	—	—	36.0
$-Br$	36.8	[27]	—	—	37.9

In the case of PMMA and PVP, just as in the case of poly(ethyleneterephthalate) [PET] and corona-treated polyethylene [PE] surfaces, the nondispersive interactions are dominant. These polymers essentially form a set with increasing degrees of polar interactions. The values of surface energies of these polymers obtained from contact mechanics measurements are listed in Tables 59.5 and 59.6. Examination of the data in these two tables shows the curious effect that all of the polymers which are dominated by dispersive force intermolecular bonding (PE, TPX, PVCH, PtBS) show relatively good agreement between the contact mechanics determined surface energy and the contact angle inferred surface energy (depending upon the model chosen for inferring the surface energy). However, the contact mechanics determined surface energy is markedly higher for those polymers which have a substantial component of nondispersive intermolecular bonding (PET, PVP, PMMA, PS, corona treated PE). The greater the nondispersive character, the greater the discrepancy between contact angle and contact mechanics determined surface energy. Lee *et al*. conjecture that the reason for the discrepancy between these two methods of determination of polymer surface energy is that the intermolecular energetics of the liquids used to determine contact angles are not the same as those in the polymer surfaces. In addition, contact angle liquids can induce changes in the substrate surface (such as rearrangement, crystallization, etc.) which would not occur for a material in contact with itself. In contact mechanics measurements, the probe of surface energy is just the material itself, thus having identical intermolecular bonding on both sides of the interface in question. However, contact mechanics measurements may cause the surface to respond by rearrangement, but possibly in a different fashion from liquid contact.

In a separate study using the JKR technique, Chaudhury and Owen [81,82] attempted to understand the correlation between the *contact adhesion hysteresis* and the phase state of the monolayers films. In these studies, Chaudhury and Owen prepared self-assembled layers of hydrolyzed hexadecyltrichlorosilane (HTS) on oxidized PDMS surfaces at varying degrees of coverage by vapor phase adsorption. The phase state of the monolayers changes from crystalline (solid-like) to amorphous (liquid-like) as the surface coverage (ϕ_s) decreases. The authors attributed the hysteresis in the case of compact monolayers to line defects and point defects formed during the vapor phase adsorption of the monolayers. The authors ruled out stress-induced rearrangement or interdigitation as a possible cause of hysteresis in these systems. It should be pointed out that the exact origins of the contact adhesion hysteresis are not well understood.

Table 59.6 gives a few interfacial-free-energy measurements against poly(dimethylsiloxane) using the JKR approach. Johnson, Kendall, and Roberts [7] give a value of 3.4 mJ/m^2 between rubber and water and Mangipudi, Tirell, and Pocius [26] give a value of 17.1 mJ/m^2 between polyethylene and poly(oxyethyleneoxyterephthaloyl). This is somewhat higher than an unattributed extrapolated melt value of 9.4 mN/m quoted by Wu [6] but in line with the value from Kasemura, Kondo, and Hata [30] of 15.4 mN/m for polyethylene/poly(oxyisophthaloyloxypropylene).

Related information can be found in Chapter 27.

TABLE 59.6. *Surface and Interfacial energies determined by JKR contact mechanics method and comparison to surface energies inferred from contact angle measurements.*

Polymer	γ_{JKR} (mJ/m^2)	γ_{SV}[a] (mN/m)	$\gamma_{PDMS\text{-}polymer}$ (from JKR technique) (mJ/m^2)	References
Poly(dimethylsiloxane) [PDMS]	21	26	0	[83]
Poly(vinyl cyclohexane)	30	32	3	[83]
Poly(4-ter-butyl styrene)	33	35	9	[83]
Polystyrene	38	39	10	[83]
Poly(*p*-phenyl styrene)	42	40	11	[83]
Poly(vinyl benzyl chloride)	43	40	12	[83]
Poly(acrylonitrile)	54	54	20	[83]
Poly(ethylenepropylene)	30	—	—	[85,86]
Poly(ethylethylene)	25	—	—	[86]
Poly(isoprene)	28	—	—	[86]

[a]Calculated from contact angle data based on Van Krevelen Group Contribution method [87].

REFERENCES AND NOTES

1. A. Couper, in Vol. IXA *of Physical Methods of Chemistry*, edited by B. W. Rossiter and R. C. Baetzold, *Investigations of Surfaces and Interfaces-Part* A (Wiley, New York, 1993), p. 1.
2. A. W. Adamson, *Physical Chemistry of Surfaces*, 4th ed. (Wiley, New York, 1982), p. 4.
3. Reference [1] is a good introduction to techniques of liquid surface tension measurement; Ref. [5] deals specifically with polymers.
4. W. A. Zisman, in *Contact Angle, Wettability, and Adhesion*, Advances in Chemistry Series No. 43, edited by F. M. Fowkes (American Chemical Society, Washington, D.C., 1964), p. 1.
5. S. Wu, *Polymer Interface and Adhesion* (Dekker, New York, 1982).
6. S. Wu, in *Polymer Handbook, 3rd* ed., edited by J. Brandrup and E. H. Immergut (Wiley, New York, 1989), p. VI/411.
7. K. L. Johnson, K. Kendall, and A. D. Roberts, Proc. R. Soc. Lond. Ser. A 324, 301 (1971).
8. D. G. LeGrand and G. L. Gaines, Jr., J. Colloid Interf. Sci. 31, 162 (1969).
9. R. H. Dettre and R. E. Johnson, Jr, J. Colloid Interf. Sci. 31, 568 (1969).
10. B. B. Sauer and G. T. Dee, J. Colloid Interf. Sci. 162, 25 (1994).
11. A. K. Rastogi and L. E. St. Pierre, J. Colloid Interf. Sci. 35, 16 (1971).
12. T. Hata and T. Kasemura, in *Adhesion and Adsorption of Polymers*, Vol. 12A *of Polymer Science and Technology*, edited by L. -H. Lee (Plenum, New York, 1980), p. 15.
13. T. C. Kendrick, B. M. Kingston, N. C. Lloyd, and M. J. Owen, J. Colloid Interf. Sci. 24, 135 (1967).
14. J. W. Belton and M. G. Evans, Trans. Faraday Soc. 41, 1 (1945).
15. G. L. Gaines Jr., J. Phys. Chem. 73, 3143 (1969).
16. G. N. Antonow, J. Chim. Phys. 5, 372 (1907).
17. M. K. Bernett and W. A. Zisman, J. Phys. Chem. 77, 2324 (1973).
18. A. G. Kanellopoulos and M. J. Owen, Trans. Faraday Soc. 67, 3127 (1971).
19. R. N. King, J. D. Andrade, S. M. Ma, D. E. Gregonis, and L. R. Brostrom, J. Colloid Interf. Sci. 103, 62 (1985).
20. R. J. Good and L. A. Girifalco, J. Phys. Chem. 64, 561 (1960).
21. F. M. Fowkes, J. Phys. Chem. 66, 382 (1962).
22. D. K. Owens and R. C. Wendt, J. Appl. Polym. Sci. 13. 1741 (1969).
23. S. Wu, J. Polym. Sci. Part C 34, 19 (1971).
24. C. J. van Oss, *Interfacial Forces in Aqueous Media* (Dekker, New York, 1994).
25. W. W. Merrill, A. V. Pocius, B. V. Thakker, and M. Tirrell, Langmuir 7, 1975 (1991).
26. V. Mangipudi, M. Tirrell, and A. V. Pocius, J. Adhes. Sci. Technol. 8, 1251 (1994).
27. M. K. Chaudhury, J. Adhes. Sci. Technol. 7, 669 (1993).
28. E. G. Shafrin and W. A. Zisman, J. Phys. Chem. 64, 519 (1960).
29. M. J. Owen, in *Silicon-Based Polymer Science*, Advances in Chemistry Series No. 224, edited by J. M. Zeigler and F. W. G. Fearon (American Chemical Society, Washington, D.C., 1990), p. 705.
30. T. Kasemura, T. Kondo, and T. Hata, Kobunshi Ronbunshu 36, 815 (1979).
31. H. Kobayashi and M. J. Owen, Makromol Chem. 194, 1785 (1993).
32. R. J. Roe, J. Phys. Chem. 72, 2013 (1968).
33. T. Kasemura, F. Uzi, T. Kondo, and T. Hata, Kobunshi Ronbunshu 36, 337 (1979).
34. J. F. Padday, in Proceedings of the 2nd International Congress on Surface Activity, Vol. 3, 1957, p. 136.
35. B. B. Sauer and N. V. Diapaolo, J. Colloid Interf. Sci. 144, 527 (1991).
36. H. Schonhorn, F. W. Ryan, and L. H. Sharpe, J. Polym. Sci. A-2 4, 538 (1966).
37. S. Wu, J. Phys. Chem. 74, 632 (1970).
38. R. J. Roe, J. Colloid Interf. Sci. 31, 228 (1969).
39. S. Wu, Org. Coat. Plast. Chem. 31(2), 27 (1971).
40. R. H. Dettre and R. E. Johnson, Jr., J. Colloid Interf. Sci. 21, 367 (1966).
41. S. Wu, J. Colloid Interf. Sci. 31, 153 (1969).
42. T. Kasemura, N. Yamashita, K. Suzuki, T. Kondo, and T. Hata, Kobunshi Ronbunshu 35, 215 (1978).
43. A. K. Rastogi and L. E. St. Pierre, J. Colloid Interf. Sci. 31, 168 (1969).
44. S. Wu, Polym. Eng. Sci. 27, 335 (1987).
45. G. W. Bender, D. G. LeGrand, and G. L. Gaines Jr., Macromolecules 2, 681 (1969).
46. S. H. Anastasiadis, J. K. Chen, J. T. Koberstein, J. E. Soho, and J. A. Emerson, Polym. Eng. Sci. 26, 1410 (1986).
47. M. Wagner and B. A. Wolf, Macromolecules 26, 6498 (1993).
48. J. J. Elmendorp and G. De Vos, Polym. Eng. Sci. 26, 415 (1986).
49. J. Hopken and M. Moller, Macromolecules 25, 1461 (1992).
50. A. G. Pittman, D. L. Sharp, and B. A. Ludwig, J. Polym. Sci. A-I 6, 1729 (1968).
51. M. K. Bernett and W. A. Zisman, J. Phys. Chem. 66, 1207 (1962).
52. D. H. Kaelble, J. Adhes. 2(4), 66 (1970).
53. M. K. Bernett and W. A. Zisman, J. Phys. Chem. 65, 2266 (1961).
54. H. Kobayashi and M. J. Owen, Macromolecules 23, 4929 (1990).
55. H. W. Fox and W. A. Zisman, J. Colloid Sci. 5, 514 (1950).
56. M. J. Owen, J. Appl. Polym. Sci. 35, 895 (1988).
57. A. H. Ellison and W. A. Zisman, J. Phys. Chem. 58, 260 (1954).
58. B. R. Ray and F. E. Bartell, J. Colloid Sci. 8, 214 (1953).
59. E. G. Shafrin and W. A. Zisman, in *Contact Angle. Wettability, and Adhesion*, Advances in Chemistry Series No. 43, edited by F. M. Fowkes (American Chemical Society, Washington, D.C., 1964), p. 145.
60. L. -H. Lee, in *Interaction of Liquids at Solid Substrates,* Advances in Chemistry Series No. 87 (American Chemical Society, Washington, D.C., 1968), p. 106.
61. H. Schonhorn and L. H. Sharpe, J. Polym. Sci. B 3, 235 (1965).

62. H. W. Fox and W. A. Zisman, J. Colloid Sci. 7, 109 (1952).
63. L. -H. Lee, J. Polym. Sci. A-2 5, 1103 (1967).
64. S. Wu, J. Phys. Chem. 72, 3332 (1968).
65. A. H. Ellison and W. A. Zisman, J. Phys. Chem. 58, 503 (1954).
66. H. W. Fox and W. A. Zisman, J. Colloid Sci. 7, 428 (1952).
67. T. Fort, Jr., in *Contact Angle, Wettability, and Adhesion,* Advances in Chemistry Series No. 43, edited by F. M. Fowkes (American Chemical Society, Washington D.C., 1964), p. 302.
68. B. R. Ray, J. R. Anderson, and J. J. Scholz, J. Phys. Chem. 62, 1220 (1958).
69. D. A. Olsen and A. J. Osteraas, J. Appl. Polym. Sci. 13, 1523 (1969).
70. N. L. Jarvis, R. B. Fox, and W. A. Zisman, in *Contact Angle, Wettability, and Adhesion,* Advances in Chemistry Series No. 43 (American Chemical Society, Washington, D.C., 1964), p. 317.
71. R. E. Baier and W. A. Zisman, Macromolecules 3, 70 (1970).
72. Y. C. Ko, B. D. Ratner, and A. S. Hoffman, J. Colloid Interf. Sci. 82, 25 (1981).
73. Y. Kitazaki and T. Hata, J. Adhes. Soc. Jpn 8, 131 (1972).
74. H. D. Feltman and J. R. McPhee, Text. Res. J. 34, 634 (1964).
75. C. J. van Oss, R. J. Good, and M. K. Chaudhury, J. Colloid Interf. Sci. 111, 378 (1986).
76. C. J. van Oss, M. K. Chaudhury, and R. J. Good, Sep. Sci. Technol. 24, 15 (1989).
77. From methylene iodide contact angle data in F. M. Fowkes, J. Adhes. Sci. Technol. 1, 7 (1987).
78. C. J. van Oss, R. J. Good, and H. J. Busscher, J. Dispers. Sci. Technol. 11, 75 (1990).
79. C. J. van Oss, M. K. Chaudhury, and R. J. Good, Adv. Colloid Interf. Sci. 28, 35 (1987).
80. From contact-angle data in C. J. van Oss, R. J. Good, and M. K. Chaudhury, J. Chromatogr. 391, 53 (1987). Note that this article quotes different calculated surface-free-energy parameters for cellulose acetate and cellulose nitrate to those in Ref. [24].
81. M. K. Chaudhury and M. J. Owen, Langmuir 9, 29 (1993).
82. M. K. Chaudhury and M. J. Owen, J. Phys. Chem. 97, 5722 (1993).
83. L. Li, V. S. Mangipudi, M. Tirrell, A. V. Pocius, NATO Science Series, II: Mathematics, Physics and Chemistry, 10 (Fundamentals of Tribology and Bridging the Gap Between the Macro- and Micro/Nanoscales), 305–329 (2001).
84. V. S. Mangipudi, and A. Falsafi in *Direct Estimation of the Adhesion of Solid Polymers*, edited by A. V. Pocius and M. Chaudhury, *Adhesion Science and Engineering, Vol. II: Surface Science* (Elsevier, Amsterdam, 2002).
85. A. Falsafi, P. Deprez, F. S. Bates, and M. Tirrell, J. Rheol. 41, 1349 (1997).
86. A. Falsafi, Ph.D. Thesis, University of Minnesota (1998).
87. D. W. Van Krevelen in *Properties of Polymers*, 3rd ed., Chapter 8 (Elsevier, Amsterdam, 1990), p. 227.

CHAPTER 60

Acoustic Properties of Polymers

Moitreyee Sinha and Donald J. Buckley

General Electric Global Research Center, One Research Circle, Niskayuna, NY 12309

60.1 INTRODUCTION

The measurement of acoustic properties of polymers, longitudinal and shear sound speeds and absorption, probe the molecular structure of polymers as well as provide a source of engineering design properties for various applications [1]. The term *acoustic* refers to a periodic pressure wave. The term includes waves in the audio frequency range (those that can be heard by the human ear) as well as those above the audio range (ultrasonic and hypersonic) and below the audio range. Acoustic waves are characterized by their sound speed and sound absorption. The sound speed C is the scalar magnitude of the sound velocity vector and has units of m/s. Sound absorption α is a measure of the energy removed from the sound wave by conversion to heat as the wave propagates through a given thickness of material. Absorption has units of dB/cm, where a dB (decibel) is a unit based on ten times the common logarithm of the ratio of two acoustic energies. Alternatively, the natural logarithm can be used, in which case the units are Np/cm, where 1 Np (neper) is equal to 8.686 dB. It is sometimes convenient to consider the amount of absorption in a thickness equal to one wavelength, λ. The quantity $\alpha\lambda$ then has units of dB (or Np). Absorption is a material property, in contrast to attenuation, which includes energy loss due to scattering and reflection as well as absorption and depends on sample size and experimental configuration.

In an unbounded isotropic solid, two types of waves can be propagated. In one case, the chain segments vibrate along the direction of propagation. This is called a longitudinal wave. In the other case, the motion of the segments is perpendicular to the direction of propagation and is called a shear wave. Longitudinal waves are also sometimes referred to as dilatational, compressional, or irrotational waves. Shear waves are also called distortional, isovoluminous, or transverse waves. These two types of waves propagate independently of one another and are the only two types possible in an unbounded, isotropic solid. The longitudinal and transverse sound speeds are related to the elastic constants by the relations

$$\begin{aligned} v_{\mathrm{l}} &= \sqrt{\frac{K + 4G/3}{\rho}}, \\ v_{\mathrm{s}} &= \sqrt{\frac{G}{\rho}}, \end{aligned} \tag{60.1}$$

where K is the bulk modulus (equal to the reciprocal of compression), G the shear modulus, and ρ the density.

For a sample whose lateral dimensions are much less than a wavelength, an extensional wave is propagated. For such a wave, the sound speed is

$$v_{\mathrm{EXT}} = \sqrt{E/\rho}, \tag{60.2}$$

where E is Young's modulus. As mentioned earlier, there are only two independent sound speeds, and the extensional sound speed can be expressed in terms of the longitudinal and shear sound speeds. It is common to express Young's modulus as a complex quantity, $E^* = E' + \mathrm{i}E''$. The ratio of the imaginary part of the modulus (Young's shear of bulk) to

the real part is the tangent of the phase angle between the two components and is called the loss factor, $\tan\delta$. The loss factor is approximately related to absorption per wavelength by the equation

$$\tan\delta = E''/E' = \alpha\lambda/\pi \tag{60.3}$$

in units of Nepers (Np). Other types of waves include surface waves and bulk waves but such waves will not be discussed here.

In viscoelastic materials such as polymers the moduli depend on frequency. Physically, the amount of deformation that is produced in a polymer by a given stress depends on the length of time that the stress is applied. In typical high frequency measurements (ultrasonic or Brillouin), during the short time that the stress of a sound wave is applied in one direction, only relatively small portions of the polymer can move; hence not as much strain is induced as in typical static or low frequency measurements, and the high frequency modulus is higher than the static modulus. Another way of looking at it is that for high frequency measurements, the time scales are so short that the distances over which the chains can relax are very short. For ultrasonic measurements, this effect is not too pronounced for the bulk modulus (on the order of 20%), but can be significant for shear and Young's modulus (a factor of 10 or more).

Because of the above dependence on frequency, sound waves represent a mechanical probe for particular wave motions, namely, motion that can occur in the period of the sound wave. Viewed as one technique for making mechanical measurements on polymers, sound wave measurements using ultrasonic or Brillouin scattering probe motions of the polymer on short length scales while methods such as audio or low frequency DMA measurements probe large-scale motions.

The different experimental methods for sound wave propagation and for measuring the mechanical response or elastic constants of polymers are summarized below with an attempt to give an idea of the different time scales involved.

Audio or ultralow frequency DMA (dynamic mechanical analysis) measurements:

1 Hz–20 kHz.

Ultrasonic experiments: 1 kHz–1 GHz.

Brillouin light scattering at hypersonic frequencies: 0.1–100 GHz.

At high frequencies (higher than 1 MHz), there is no direct way to measure the modulus by applying known values of stress and measuring the strain. At these frequencies, the elastic constants for polymers are calculated from sound velocity measurements using ultrasonic or Brillouin light scattering experiments. In this review, we will largely focus on measurements at ultrasonic frequencies. For elastomeric networks we will briefly review sound wave measurements reported at very low frequencies and at very high (GHz) frequencies.

The propagation of a sound wave is fundamentally a molecular process, and the interaction between elastic wave propagation and molecular behavior has a significant effect on sound dispersion and attenuation, particularly at ultrasonic frequencies. If a sound wave in a fluid disturbs any particular equilibrium molecular aggregation, it takes a certain time t, called the relaxation time, for the original state to be restored after the passage of the crest of the wave. The process is usually called thermal relaxation.

As is well known for viscoelastic materials, the frequency and temperature dependencies of polymer properties are related. For groups of relaxation processes that encompass a very broad time range, it often happens that the experimentally limited frequency range is not large enough to obtain a complete curve. Using the time–temperature superposition principle, measurements carried out at a sequence of different temperatures can provide the missing information to generate the frequency-dependent curve as shown in Fig. 60.1 [2].

60.2 LOW FREQUENCIES

At the lower frequency end (less than 20 kHz), there have been some earlier studies on sound or pulse propagation in rubbery polymers. Some related work on natural and butyl rubber is discussed below.

Witte *et al*. reported velocity and attenuation measurements in thin strips of butyl rubber from 0.5 to 5 kHz (audio frequency) at different temperatures [3]. They found the speed of sound to increase with decreasing temperature and increasing frequency. The attenuation showed a peak with temperature. The experimental procedure made use of a signal generator for driving a crystal, setting up longitudinal waves which were transmitted through the sample and picked up by a crystal receiving element. Thus it was possible to determine the phase difference between the driven end and the pickup for any point along the sample. By

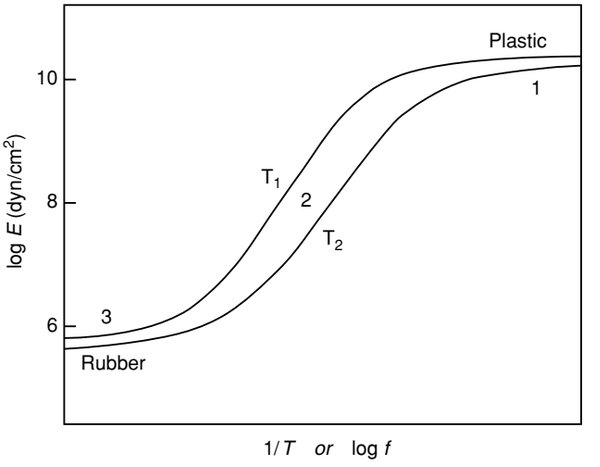

FIGURE 60.1. Rubber to glass transition at two temperatures ($T_1 < T_2$) [2]. Reprinted with permission from J. D. Ferry, Viscoelastic Properties of Polymers, 3rd ed. (1980). Copyright 1980, Wiley.

moving the pickup along the sample, the distance between two adjacent points in the same phase of motion were measured, and thus the wavelength of the sound wave in the sample could be determined. Knowing the frequency of the driving oscillator, the velocity was directly obtained. The attenuation was obtained by moving the pickup along the sample and reading on the wave analyzer, the amplitude of the received signal as a function of distance. This method of measurement is limited to a definite frequency range; an upper limit to the frequency range is determined by the fact that the largest cross-sectional dimension of the sample had to be kept small in comparison with the wavelength of the propagated wave. At sufficiently low frequencies, the sample length became smaller than the half-wavelength of the transmitted sound wave making velocity measurements impossible.

Figure 60.2 shows the velocity curves of butyl rubber as a function of frequency at different temperatures. The velocity increases very slowly with frequency at high temperatures where the values of the velocity are of the order of 40 m/s. The increase in velocity with frequency is much more rapid as the temperature is lowered, and at 0 °C the velocity is about 300 m/s. The corresponding modulus curves derived from the velocity curves is shown in Fig. 60.2. At all temperatures the modulus was seen to increase with frequency. From ultrasonic experiments on the same polymers, the data obtained at frequencies in the MHz range indicated a continuous rise in the modulus with frequency (measured up to 15 MHz). The dispersion over a limited frequency range can be attributed to a mechanism involving relaxation times of the order of $1/\omega$, whereas the entire dispersion range would have to be explained on the assumption of a wide distribution of relaxation times. The relaxation mechanism for these low frequency measurements responsible for the dispersion would involve the assumption of a number of relaxation times of the order of 10^{-3}s. Also from their results they found that an increase in temperature produced the same effect as a decrease in frequency. This supports the time–temperature superposition principle for viscoelastic materials.

Gent and Marteny [4] measured the difference in time for loading and unloading pulses to reach two phonograph pickups, placed a known distance apart, to determine the velocity of sound as a function of strain in filled and unfilled natural rubber. For both cases they found a marked increase in the speed of sound with imposed strain. For the unfilled rubber, the sound velocity increased from about 60 m/s at zero strain up to about 600 m/s at high strains (about four times the original length) (Fig. 60.3). For the filled rubber, the speed was about 160 m/s at zero strain and reached about 800 m/s at high strains.

Although wave propagation techniques have been used extensively to study the bulk properties of polymers, their application in understanding the microscopic structure of networks has been limited. Most of the studies have been directed toward studying the change in sound velocity with temperature and frequency, or toward the determination of various bulk properties such as the modulus, hysteresis, absorption, etc. of networks. The nonlinear nature of the elastic material carrying the disturbance has been treated in a phenomenological manner. Sinha *et al*. measured the speeds of longitudinal and transverse pulses in uniaxially stretched siloxane (PDMS) networks as a function of the extension ratio, the degree of crosslinking and the amount of swelling [5]. They used a theoretical framework combining the theory of elastic wave propagation and molecular models for the networks to determine network parameters from measurements of the wave velocity in deformed

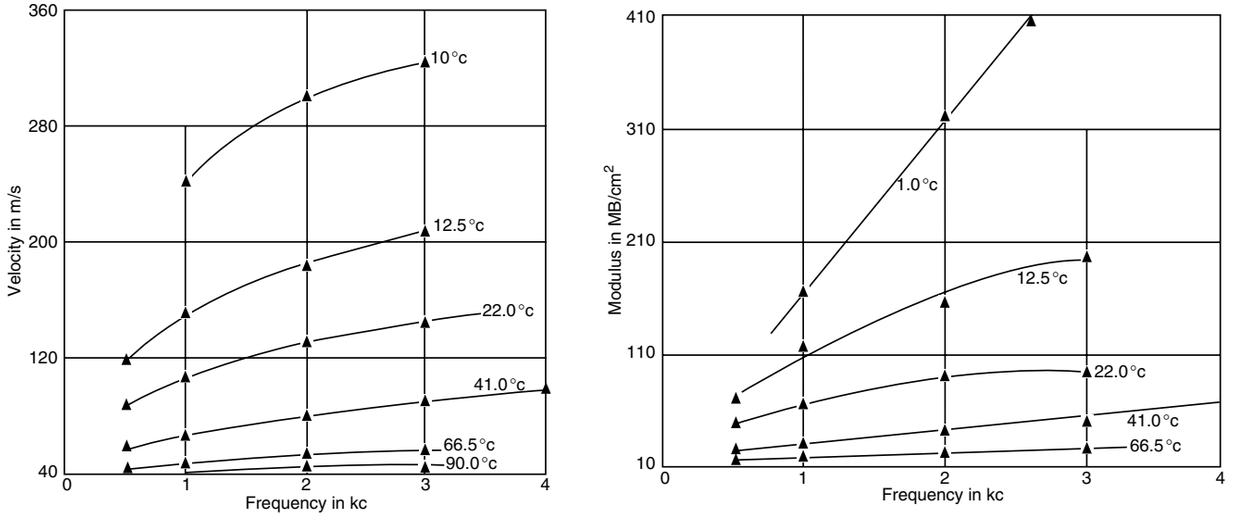

FIGURE 60.2. Velocity versus frequency for butyl rubber. The dynamic Young's modulus as a function of frequency for butyl rubber [3]. Reprinted with permission from R.S. Witte, B.A. Mrowca, and E. Guth, Journal of Applied Physics, 20, 481 (1949). Copyright 1949, American Institute of Physics.

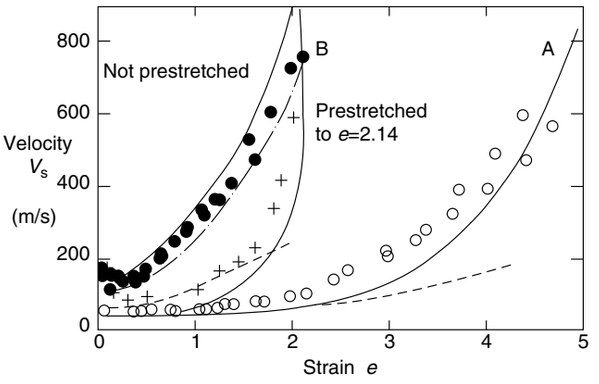

FIGURE 60.3. Velocity of sound for unfilled rubber (open circles) and in carbon-black filled rubber (filled circles); Velocity in filled rubber after prestretching to a strain value of 2.14 (crosses). Full curves: calculated from values of the instantaneous modulus obtained from unloading stress–strain relations. Broken curves: calculated using loading stress–strain relations. Chain curve: calculated using loading-after-resting stress–strain relations [4]. Reprinted with permission from A.N. Gent and P. Marteny, Journal of Applied Physics, 53, 6069 (1982). Copyright 1982, American Institute of Physics.

networks. From ultrasonic measurements on PDMS [6], the values reported for the longitudinal speed is 1,020 m/s using an immersion measurement technique based on measuring the differences between acoustic paths with and without the specimen. This corresponds to a longitudinal elastic modulus of 1.087 GPa, about 10^4 times higher than the equilibrium modulus.

60.3 ULTRASONIC FREQUENCIES

60.3.1 Ultrasonic Material Properties

The term ultrasound in its broadest sense covers all sound with frequencies greater than the audible range. In general use, however, the term is restricted to frequencies of 1 MHz and greater, up to the point where phonon processes, such as Brillouin scattering, become important.

Ultrasonic investigations are often performed using the immersion technique where the sample and transducer (a combined transmitter and receiver of ultrasonic radiation) are immersed in a liquid, typically water, although other fluids such as silicone oil may be used. The fluid supplies efficient coupling of ultrasonic energy between the output lens of the transducer, which is typically a hard thermoplastic such as polystyrene, and the sample. In another arrangement, energy is coupled directly to the sample in that a pulse propagates from the transducer through a thin layer of coupling medium (usually soapy water to assure good wetting of the polymer surface) into a plane polymer sample.

Both methods use the pulse–echo technique. A pulse is sent into the sample, where it is reflected by the front and back surfaces of the material and returned at reduced amplitude to the transducer, while the waveforms are monitored on a recording oscilloscope. From the timing and amplitude of the reflected waves the sound speed and attenuation of the material may be determined. Successive reflections provide additional information on both these properties. A typical ultrasound pattern obtained using the direct-coupled transducer method is shown in Fig. 60.4.

Normal Incidence

The longitudinal sound speed in the polymer can be determined by measuring the time required for a pulse propagated normally into the sample to reflect from its far surface (usually a polymer/air interface where the impedance mismatch generates a reflected wave), and dividing the sample's thickness by twice this time. The time is determined by the interval between the initial pulse and the successive reflections, which result as the wave bounces

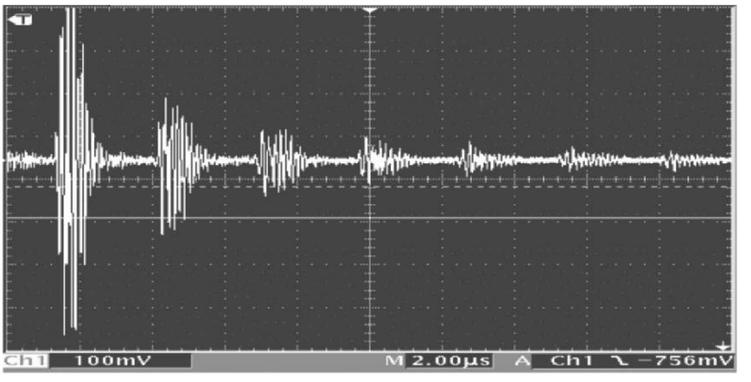

FIGURE 60.4. Ultrasound pulse–echo pattern obtained at 10 MHz in a polystyrene disk 3 mm thick. The interval between successive reflections indicates the velocity of the longitudinal wave, and the ratio of intensity of any two successive reflections the attenuation. The horizontal scale is 2.00 μs/division. In this material the (longitudinal) speed of sound is 2.14 km/s, the acoustic impedance is 2.25 MRayls (units of 10^6 kg/(cm^2-s) and the attenuation coefficient is ca. 12 db/cm. See text below for the calculation [57].

off the water/plastic interface repeatedly. The velocity is then

$$C_L = 2d/t. \tag{60.4}$$

In the example in Fig. 60.4, $d = 3$ mm, $t = 2.8$ μs, and C_L is 2.14 mm/μs or 2.14 km/s.

From the same trace, the longitudinal absorption coefficient can be determined by observing the peak height in successive reflected pulses. The attenuation per unit length is usually expressed on a logarithmic scale in units of decibels/cm (abbreviated dB/cm), where the decibel represents a reduction in power of 1.258 times. The attenuation is then:

$$\alpha(\text{dB/cm}) = 10/L \log (I_{\text{initial}}/I_{\text{final}}) \tag{60.5}$$

or, in terms of the voltages (signal amplitudes) displayed on an oscilloscope,

$$\alpha = 20/L \log (V_{\text{initial}}/V_{\text{final}}), \tag{60.6}$$

where V_{initial} is the pulse height going in, V_{final} the height coming out, and L the path length in the sample, equal to twice the thickness.

In addition to attenuation within the sample, there are losses from reflection at the sample/air and sample/coupling medium interfaces, and losses in transversing the coupling. The latter are small in the direct-coupled technique, but can be significant in the immersion tank method. The former can be significant to the extent of mismatch of the acoustic impedances of the two media. The acoustic impedance Z, a quantity analogous to the electrical impedance, is the product of the sound velocity and the density, expressed in units of megaRayls, MRayls or 10^6 kg/(s m^2). For example, the impedance mismatch of polystyrene (Z=2.5 and a material often used for transducer lensing) with water (Z=1.5) results in a portion of the incident beam being reflected, that portion having amplitude:

$$\begin{aligned} R_{\text{PS-Water}} &= [(Z_{\text{PS}} - Z_{\text{Water}})/(Z_{\text{PS}} + Z_{\text{Water}})] \\ &= [(2.5 - 1.5)/(2.5 + 1.5)] = 0.25 \end{aligned} \tag{60.7}$$

and the reflected intensity is

$$R^2_{\text{PS-Water}} = [0.25]^2 = .064. \tag{60.8}$$

The equivalent calculation for the air/polystyrene interface gives

$$R^2_{\text{PS-Air}} = 0.186. \tag{60.9}$$

Generally, sound velocities are much more readily and accurately measured than absorption coefficients, since only time differences are required for the former, while measurement of the latter are influenced by many artifacts, such as the reproducibility of the coupling, beam spread and dispersion.

Oblique Incidence

When the transducer beam is not normal to the sample surface, both longitudinal and shear waves are generated. The longitudinal wave may be eliminated by increasing the incident angle until total internal reflection of this component occurs, at the critical angle given by Snell's law,

$$\sin \theta_P / C_P = \sin \theta_m / C_m, \tag{60.10}$$

where the medium (m) of the incident wave is often a prism of polystyrene or polymethylmethacrylate (PMMA). For a polystyrene prism with $C_P = 2.4$ m/s, propagating into a PMMA slab with $C_P = 2.7$ m/s the critical angle is approximately 51 °.

Owing to the non-normal incidence, measurement of the shear wave velocity C_s requires a separate transmitter and receiver. The path length in the specimen is given by [43]:

$$x = L[1 - [C_s \sin \theta C^2_m]^{-1/2} \tag{60.11}$$

and the shear velocity C_s by [43]:

$$C_s = C_m\{[\cos \tilde{\theta} C_m \Delta t/L]^2 + \sin^2 \theta\}^{-1/2}. \tag{60.12}$$

Shear and Bulk Moduli

Ultrasound can also be used to determine the elastic moduli of materials, with the modulus of interest determined by the mode of propagation: longitudinal (sound waves producing motion of sample's atoms parallel to the direction propagation), shear (excitation at right angles to the direction of propagation) and extensional (longitudinal excitation in the sample with lateral dimensions small compared to the ultrasonic wavelength).

The speed of sound C for a given propagation mode is related to the corresponding modulus M and the density ρ by the general relation [2]

$$\rho C^2 = M. \tag{60.13}$$

For a longitudinal and shear waves, respectively, the relations are [43]:

$$\begin{aligned} \text{Longitudinal: } \rho C^2_{\text{Longitudinal}} &= K + 4/3G, \text{ Shear:} \\ \rho C^2_{\text{Shear}} &= G, \end{aligned} \tag{60.14}$$

where K and G are the bulk and shear moduli, respectively. At low frequencies, where the wavelength can be greater than the lateral dimension of the sample, there is a third mode, extension, where the relation is

$$\rho C^2_{\text{Extensional}} = E \tag{60.15}$$

with E being the Young's modulus. Typical sound velocities in materials are or order 2–5 × 10^2 for gases, 1–3 × 10^3 for organic solids, and 3–6 × 10^3 for dense crystalline solids. The frequencies of interest for applied ultrasound are in the range 1–100 MHz, corresponding to wavelengths of 2–0.02 mm when propagating in polystyrene. The shear velocities are typically (1/3)–(1/2) those in the longitudinal mode.

Longitudinal waves may be generated using a piezoelectric transducer activated by an RF pulse train of the

appropriate frequency, with the transducer coupled at normal incidence to the sample surface. Shear and longitudinal waves can be generated in a sample using the same equipment but with the transducer face oriented at angle from normal using a plastic coupling wedge.

Tables 60.1 and 60.2 list values of the longitudinal and shear velocities at 1 MHz, and attenuations at 2 MHz at room temperature for some common polymers [2].

Temperature, Frequency and Pressure Dependence of Ultrasonic Properties

The largest change in acoustic properties of a polymer occurs across T_g, when the material transitions from a hard glassy solid to the rubbery plateau. Above this temperature the moduli and sound speeds drop (a rule of thumb for the latter is that it decreases by a factor of 2) while the absorption increases by an order of magnitude or more, with a maximum some distance above T_g. The temperature derivatives are maximum around T_g and are of order 25 m/s/K [2].

Since there is a time–temperature superposition for polymers, the frequency and temperature dependences of the acoustic properties are inversely related, so that decrease in temperature correspond to the effect of increases in frequency. This behavior is illustrated by comparing Fig. 60.5(a) and (b) which display the temperature and frequency sensitivity for two polymers [1]. Since measurements over a wide temperature range are more readily made than those over a corresponding frequency range, the combination of the data from measurements over a wide temperature range and a modest frequency range usually serve to define the entire spectrum. The frequency sensitivity of ultrasound velocities is weak, of order 5–10 m/s/decade [2]. The attenuation, however, is strongly dependent, increasing at least linearly and often as the square of frequency, and is of order 20–100 dB/cm/decade. For example, over the range 4–6 MHz, the speed of longitudinal sound in PMMA changes by only 1%, [52] while the attenuation increases from 40 to 60 Nps/m. Both velocity and attenuation are sensitive functions of temperature, with velocity decreasing across T_g to ca. 1/2 its low temperature plateau value, while attenuation peaks at or near T_g.

The pressure derivative of the sound speeds are inversely related to temperature since a pressure change results in a change in free volume. Few pressure derivatives have been measured; typical values are of 0.5–0.9 GPa^{-1}.

49.3.2 Applications of Ultrasound for Polymers

Acoustic Dynamic Mechanical Analysis (DMA)

At acoustic frequencies, the attenuation goes through a maximum determined by the spectrum of relaxation times in the polymer; hence dynamical mechanical analysis can be performed by scanning over a wide frequency range, typically $10^3 - 10^{12}$ Hz. An example of the technique is sonic DMA of PVC [54] which shows that the shear modulus increase monotonically with frequency, while the longitudinal or extensional modulus displays the transition associated with T_β. The ratio of the loss and storage moduli, or tan delta obtained via DMA can be related to the absorption coefficient through the equation [2]:

$$\alpha = \Pi\lambda \tan\delta = \Pi\lambda E''/E'. \qquad (60.16)$$

TABLE 60.1. *Longitudinal and shear velocities for common polymers at 25 °C and 1 MHz [1].*

Acronym	Poly-	Density (g/cm^3)	C_L (m/s)	C_s (m/s)	References
ABS	acrylonitrile–butadiene–styrene	1.041	2,160	930	[30]
Epoxy	DGEBA/PDA	1.184	2,890	1,290	[34]
Nylon	hexamethylene adipamide	1.147	2,710	1,120	[6]
PC	carbonate	1.194	2,220	909	[28]
PE	ethylene	0.957	2,430	950	[6]
PEO	ethylene oxide	1.208	2,250	—	[6]
PES	ether sulfone	1.373	2,260	—	[29]
Phenolic		1.220	2,840	1,320	[25]
PMMA	methylmethacrylate	1.191	2,690	1,340	[6]
PMP	methyl pentene	0.835	2,180	1,080	[30]
POM	oxymethylene	1.425	2,440	1,000	[6]
PP	propylene	0.913	2,650	1,300	[6]
PPO	phenylene oxide	1.073	2,220	1,000	[28]
PS	styrene	1.052	2,400	1,150	[6]
PSU	sulfone	1.236	2,260	920	[28]
PVC	vinyl chloride	1.386	2,330	1,070	[29]
PVDF	vinylidene fluoride	1.779	1,930	775	[6]
Silicone	dimethylsiloxane	1.045	1,020	—	[6]
Teflon	tetrafluoroethylene	2.180	1,410	730	[33]
Urethane	polyol/TDI/ TMAB	1.118	1,750	—	[39]

TABLE 60.2. *Longitudinal and shear absorption coefficients for polymers at 25 °C & 2 MHz[1].*

Acronym	Polymer	ρ (g/cm^3)	α_L (dB/cm)	α_S (dB/cm)	References
ABS	Poly(acrylonitrile–butadiene–styrene)	1.02	1.8	15	[30]
Epoxy	DGEBA/PDA	1.1844	6.3	36.1	[34]
Epoxy	BGDE/PDA	1.179	21.0	—	[37]
Nylon 6	Polycaprolactam	—	13	—	[41]
PC	Polycarbonate	1.19	9.4	—	[29]
PMMA	Poly(methylmethacrylate)	1.19	1.4	4.3	[42]
PE	Polyethylene	0.96	3.3	25	[42]
PE	Polyethylene	—	13	—	[41]
PEO	Poly(ethyleneoxide)	1.21	7.1	—	[42]
PES	Poly(ethersulfone)	1.37	5	—	[29]
Phenolic		1.22	4.1	19	[25]
PIB	Polyisobutylene	0.91	67	—	[32]
PMP	Poly(4-methyl-1-pentene)	0.84	1.4	6.7	[30]
PS	Polystyrene	1.40	—	—	[41]
PS	Polysulfone	1.24	4	—	[29]
PU	Polyurethane, polyether based	1.104	7.5	—	[43]
PU	Polyurethane, polybutadiene based	1.008	9.1	—	[43]
PVC	Poly(vinylchloride)	—	8.1	—	[41]

Polymers for Medical Ultrasonic Devices

The optimal polymer material for use in ultrasound medical devices would have an impedance matching that of human tissue, 1.5 MRayls, and minimal attenuation at the frequencies of interest, which are typical between 5 and 10 MHz. Use of a material with a large impedance mismatch against tissue results in reflection of energy at the tissue/transducer interface, or more likely, the interface between the coupling gel, which is often silicone or a hydrogel, and the device lens. A polymer with an impedance mismatch and low attenuation can result in multiple reflections within the subject and consequent reduction of signal-to-noise in the image.

Hard, glassy, brittle thermoplastics such as polystyrene (PS) and polymethylmethacrylate (PMMA) have low attenuations, of order 6–10 dB/cm at 10 MHz, and in the case of PS, a low acoustic impedance. Ductile polymers such as polycarbonate (PC), many polyolefins and impact-modified thermoplastics generally have high absorption coefficients, in the range 20–40 dB/cm. The same molecular structures and mobility, which contribute to ductility, may also contribute to absorption of ultrasonic energy. Not surprisingly, rubbers and, by extension, any polymer above its

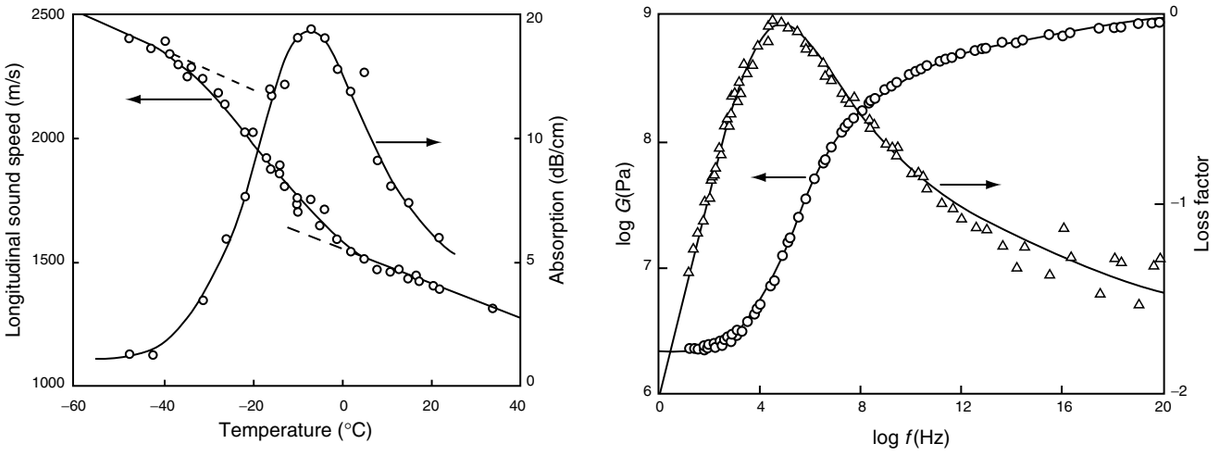

FIGURE 60.5. (a) Sound speed and absorption vs. temperature for poly (carborane siloxane) and (b) log plot of shear modulus and loss factor vs. frequency for polyurethane [1]. Reprinted from [1] Copyright 1996, with permission of Springer Science + Business Media.

glass transition temperature, are highly attenuating materials at all frequencies. The requirement of impedance match, low attenuation and reasonable mechanical properties (strength, toughness, etc.) limits the choice of available polymers for ultrasonic uses such as mammography compression paddles. In this application polymethylpenetane, a low-density polyolefin, has proven useful. This material has impedance of 1.7 MRayls and an absorption coefficient of 6 dB/cm at 10 MHz, and is a good compromise mechanically between brittle materials used in ultrasonic lenses, such as PS, and more ductile but highly absorbing polymers such as PC.

Acoustic Emission

When subjected to stresses sufficient to initate and propagate cracks, polymers emit sound waves with frequencies ranging from the upper acoustic limit (ca. 10 kHz) to 10 MHz that may be detected with suitable transducers. A well-isolated acoustic emission (AE) system may used to detect deformation events including the slow to fast brittle crack transition in PMMA, fatigue in SEN samples, and crack propagation under high hydrostatic pressure [53].

Sono-Chemistry

Ultrasound has also been employed to accelerate chemical reactions, including breakdown of polymers in solution, and catalytic reactions [55]. Ultrasound is capable of producing high local temperatures and pressures unlike any other apparatus, and can drive unique chemistries as a result. The principle mechanism is cavitation of the sonic agitated fluid and the resulting bubbles collapse/explode at surfaces, which in turn produce high velocity microjets of liquid. This produces both physical and chemical changes.

An example of sono-chemistry is degradation of high molecular weight PS and reaction of the low molecular weight block with MMA monomer to produce a PS-PMMA block copolymer [55]. Another example is surface modification of Polyethylene using moderate oxidizing agents to improve adhesion and wetability [55].

Ultrasonic Shear Rheology

Ultrasound can also be used to explore the viscoelastic properties of polymers in film form. Alig *et al*. [56] describe a shear rheometer operating in the range 1–40 MHz. on the shear reflection principle. A shear wave is sent through a quartz bar toward the interface between the bar and a polymer film. The film alters both the amplitude and phase of the reflected wave. The values of G' and G'' obtained when plotted against offset temperature from T_g (i.e., $T - T_g$), show broader transitions at higher temperatures than those obtained with low frequency mechanical DMA. One advantage of the ultrasound method is that it allows DMA of materials, which would be unsuitable for conventional DMA, such as latex dispersions, gels, and mechanically fragile films.

60.4 HYPERSONIC (GHZ) FREQUENCIES

Brillouin scattering measurements provide the velocity and attenuation of acoustic phonons having frequencies in the range of GHz and wavelengths of the order of 10^3Å [7]. Laser light of frequency ω_i and wave vector $\bar{k}_i$ is incident on the sample; the light interacts with the medium and is scattered through an angle θ. Phonons are absorbed or emitted in the inelastic light scattering process governed by the following energy and momentum conservation equations

$$\begin{aligned} \omega_s &= \omega_i \pm \Delta\omega, \\ \bar{k}_s &= \bar{k}_i \pm \bar{k}, \end{aligned} \tag{60.17}$$

where $\bar{k}_s$ and $\bar{k}$ are the wave vectors of the scattered laser light and the phonon, respectively. Likewise ω_i and $\Delta\cdot\omega$ are the frequencies of the scattered light and the phonon.

The basic experiment consists of measuring the spectrum of the scattered light. It consists of a strong elastic peak at one frequency with additional components whose frequency has been shifted by the inelastic scattering processes. The frequencies of these much weaker phonon peaks are measured relative to the elastic peak. From observation of the shifted Brillouin peak with respect to the central elastic peak, the longitudinal Brillouin splitting, $\Delta\omega_l$ is given by

$$\Delta\omega_l = kv_l, \tag{60.18}$$

where v_l is the longitudinal phonon velocity with wave vector $k = (4\pi n/\lambda_i)\sin(\theta/2)$, n is the refractive index of the material, λ_i is the wavelength of the incident light in vacuum. The longitudinal sound velocity, v_l depends on the real part of the longitudinal viscoelastic modulus. It can be expressed in terms of the longitudinal elastic modulus, M as shown

$$v_l = \sqrt{M/\rho} = \sqrt{(K + 4G/3)/\rho}, \tag{60.19}$$

where K is the bulk modulus and G is the shear modulus [8]. The line-width of the Brillouin peak measures the attenuation of the acoustic phonon. The Brillouin peaks are predicted to have a half-width at half-maximum, Γ given by

$$\Gamma = \frac{2}{3}\frac{q^2\eta}{\rho}, \tag{60.20}$$

where η is the longitudinal viscosity and Γ is measured in hertz.

For linear PDMS, Brillouin scattering measurements on two molecular weights of PDMS (3,800 and 68,000) by Patterson *et al*. exhibited no measurable difference in the phonon speed [9]. It was concluded that the asymptotic

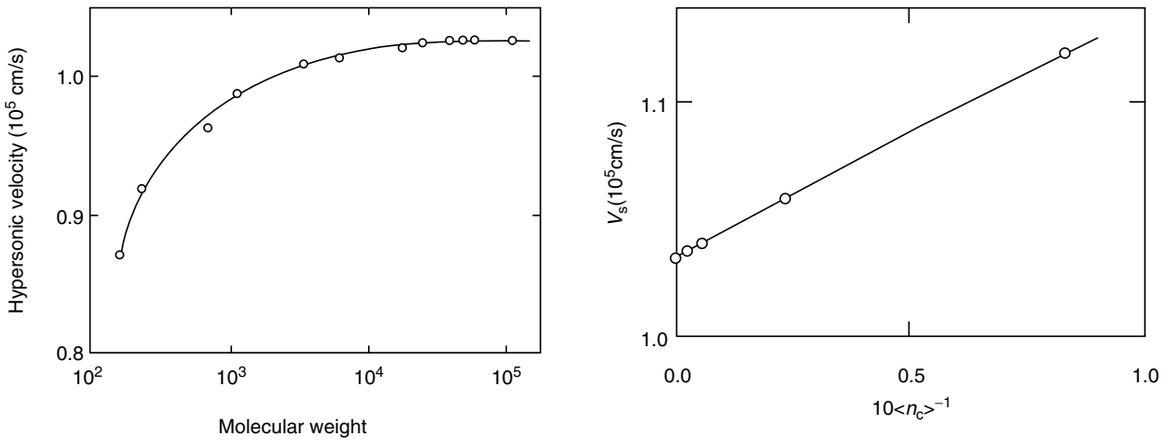

FIGURE 60.6. (a) Phonon velocity in linear polydimethylsiloxane as a function of the molecular weight. (b) Phonon velocity in rubbery PDMS as a function of cross-link density. Here n_c is the average number of monomer units between cross-links and is directly proportional to M_c [11]. Reprinted with permission from Shingo Kondo and Takashi Igarashi, Journal of Applied Physics, 51, 1514 (1980). Copyright 1980, American Institute of Physics.

leveling of the phonon speed happened below the lower number-averaged molecular weight of 3,800 g/mol. The samples used in this case were highly polydisperse. Kumar [10] and Kondo *et al*. [11] reported that the phonon velocity in linear PDMS increased with increasing molecular weight and had a tendency to level off in the region of higher molecular weight of around 7,000 g/mol (Fig. 60.6 (a)). For cross-linked networks, Lindsay *et al*. found the elastic modulus M to increase linearly with increasing cross-link density [12]. These were reported as preliminary results carried out on networks formed by random cross-linking using γ irradiation. Kondo and Igarashi reported the phonon velocity and modulus to increase linearly with cross-link density for networks with four molecular weights prepared by an addition reaction (Fig. 60.6 (b)) [11]. Kondo *et al*. also reported measurements on end-linked networks that were highly cross-linked and had much higher phonon speeds [13]. Delides *et al*. [14] measured average values of 1,040 $\pm$ 20 m/s, while Kondo and Igarashi reported values from 1,240 to 1,280 m/s. Wang *et al*. examined the effect of the relaxation of longitudinal stress modulus on the propagation behavior of the thermally driven acoustic wave in siloxanes [17]. Patterson reported the hypersonic attenuation in amorphous PDMS was studied as a function of temperature and pressure [7]. Kondo *et al*. investigated Brillouin scattering from networks of end-linked dimethylsiloxanes to study the hypersonic loss processes [13]. Figure 60.7 summarizes their findings. Here the attenuation $\alpha\lambda_s$ is defined as

$$\alpha\lambda_s = \pi\frac{2\Gamma}{\nu_p}, \tag{60.21}$$

where α is the attenuation per wavelength. The x-axis has been chosen as inverse of the number of skeletal elements $(2n + 5)$ with $n = 1, 2, 3, 4, 5$, and 6. This corresponds to extremely highly cross-linked networks with $M_c = 274$–644 g/mol. The hypersonic attenuation attained a maximum at $n = 4$–6. The hypersonic frequency shows a steep decrease with increasing chain length and decreases by about 45%. Since the refractive index changes only by about 2% for the different molecular weight samples, this would imply a very dramatic change in the phonon velocity.

Brillouin spectroscopy can also be used to study the change of sound velocity with deformation. Anders *et al*. reported the longitudinal sound velocity in stretched poly (urethane) and poly (diethylsiloxane) (PDES, Figure 60.8) networks [15]. They used the lattice-model to determine the force constants [11]. The samples showed different deformation-dependent behavior of the force constants. For the

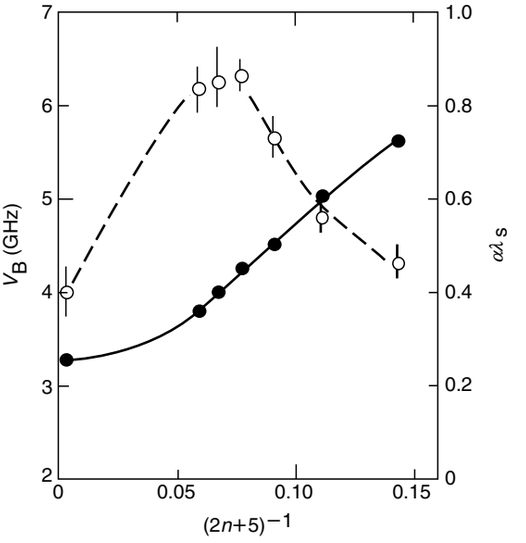

FIGURE 60.7. Phonon frequency (filled circle) and attenuation (empty circle) in highly cross-linked rubbery PDMS as a function of the number of skeletal elements. The hypersonic attenuation attains a peak for $n = 4$–6 [13].

diol-extended polyurethanes, the longitudinal sound velocity increased in the direction of stress and decreased in the direction perpendicular to it. The diamine-extended polyurethanes showed anomalous behavior. While the sound velocity increased parallel to the stress direction as expected, it also increased along the direction perpendicular to the stress. For the PDES samples, they found in some cases no significant variation of the sound velocity while in the other cases they found the same anomalous behavior as observed in the polyurethanes. Sinha *et al*. reported the molecular weight dependence of the phonon speed for a series of nearly monodisperse PDMS networks [16]. They showed that, at sufficiently low cross-link densities, the longitudinal phonon speed in these networks approaches the speed in uncross-linked high molecular weight PDMS liquids.

In comparing elastic constants measured ultrasonically or from Brillouin scattering with those observed in a ''static'' (very low frequency measurement), it is important to note that the ultrasonic/Brillouin values are adiabatic while static values are isothermal. In elastomers, the acoustic response is largely determined by the network structure introduced by chemical cross-linking. The mechanical behavior at higher frequencies (in the GHz regime) may have a very small molecular dependence, depending on the frequency at which the rubber–glass transition occurs for PDMS (Fig. 60.1). For PDMS networks [16], the change in modulus as a function of cross-link density in equilibrium measurements is considerably higher than that observed in Brillouin scattering measurements (about 90% decrease in modulus for $M_c = 4{,}000$–$40{,}000\,\mathrm{g/mol}$ in equilibrium measurements). The decrease in speed for the same range of molecular weights was found to be about 75% using the low frequency sound waves [5] compared to the 10% decrease at the GHz frequencies [16]. At GHz frequencies, when a stress is exerted in a particular place in the sample, the distance over which relaxations can occur is very short. The dependence of the modulus on the chain length between cross-links is therefore much less compared to low frequency measurements where there the time scales are much larger and therefore the chains can relax over longer length scales. At these frequencies, in Brillouin scattering experiments, the sound wave propagation of a polymer therefore depend primarily on the intermolecular potential, which is a function of intermolecular separation and hence volume. Thus there will be a change in the phonon velocity whenever there is a change in any physical property that affects volume, such as crystallinity, cross-linking, and plasticization.

60.5 CONCLUDING REMARKS

In order to have a more complete understanding of the acoustic properties of polymers, it is desirable to probe the response over as wide a range in frequency as possible. In the low frequency range (kHz), the propagation of an externally generated mechanical disturbance is used to measure the acoustic properties. In the high frequency hypersonic range (GHz), intrinsic thermal phonons using Brillouin scattering are used to measure the acoustic properties. In the ultrasonic (MHz) frequency range, which lies in between these two limits, propagation of externally excited sound waves is used to study amorphous polymeric medium. Collectively, results from these different measurement techniques can provide information about the mechanical behavior of polymers over a wide range of time scales.

ACKNOWLEDGMENTS

The authors would like to acknowledgment the contribution of Dr. Bruce Hartmann, now deceased, who was the author of the chapter on acoustical properties published in the previous edition of this handbook. Dr Hartmann's comprehensive work provided the starting point for this article.

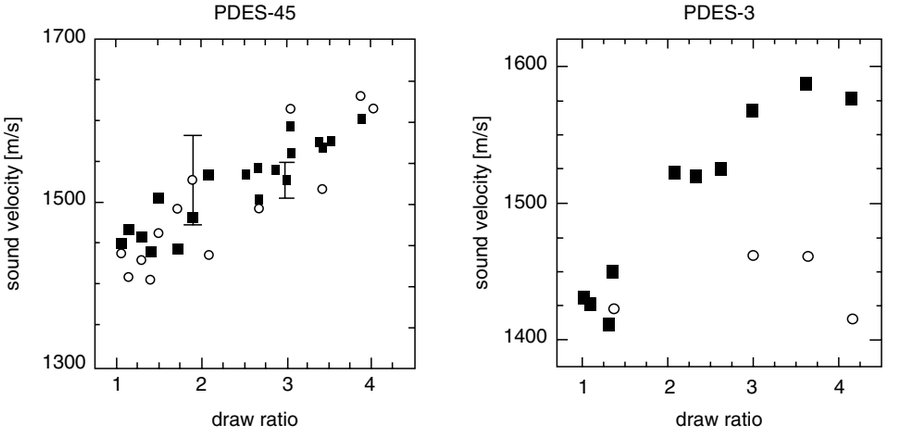

FIGURE 60.8. Sound velocity of the longitudinal polarized phonon measured parallel (filled squares) and perpendicular (empty circles) to the draw direction measured by Brillouin scattering. The samples are polydiethylsiloxanes with $M_n = 45{,}000$ and 43,000 labeled as PDES-45 and PDES-3, respectively [15]. Reprinted from S.H. Anders, H.H. Krbecek, and M. Pietralla, J. Polym. Sci., Polym. Phys. Ed. 35, 1661-1676 (1997). Copyright 1997, with permission of Wiley-VCH.

REFERENCES

1. B. Hartmann, *Physical Properties of Polymers Handbook*, ed. J. E. Mark, Chapter 49 (American Institute of Physics Press, 1996).
2. J. D. Ferry, Viscoelastic Properties of Polymers, 3rd. ed. (Wiley, New York, 1980).
3. R. S. Witte, B. A. Mrowca, and E. Guth, J. Appl. Phys. 20 (6), 481 (1949).
4. A. N. Gent and P. Marteny, J. Appl. Phys. 53(9), 6069–6075 (1982).
5. M. Sinha, J. E. Mark, B. Erman, T. H. Ridgway, and H. E. Jackson, Macromolecules 36, 6127–6134 (2003).
6. B. Hartmann and J. Jarzynski, J. Acoust. Soc. Am. 56, 1469 (1974).
7. G. D. Patterson in *Methods of Experimental Physics*, vol. 16, Part A, p. 170, ed. R. A. Fava (Academic Press, New York, 1980).
8. G. D. Patterson, J. Polym. Sci., Polym. Phys. Ed. 15, 455 (1977).
9. G. D. Patterson, Macromolecules 17, 885–888 (1984).
10. A. Kumar, Univ. Microfilms, Ann Arbor, Mich., Order No. 74–13, 926; through Diss. Abstr. Int. B 34 (no. 12), 6033 (1974).
11. S. Kondo and T. Igarashi, J. Appl. Phys. 51(3), 1514–1519 (1980).
12. S. M. Lindsay, A. J. Hartley, and I. W. Shepherd, Polymer 17, 501 (1976).
13. S. Kondo and T. Igarashi, Polymer 24 (Commun.), 221 (1983).
14. C. G. Delides and A. C. Stergiou, Polymer 26 (Commun.), 168 (1985).
15. S. H. Anders, H. H. Krbecek, and M. Pietralla, J. Polym. Sci., Polym. Phys. Ed. 35, 1661–1676 (1997).
16. M. Sinha, J. E. Mark, H. E. Jackson, and D. Walton, J. Chem. Phys. 117(6), 2968 (2002).
17. C. H. Wang, Q. L. Liu, and B. Y. Li, J. Polym. Sci., Polym. Phys. Ed. 25, 485 (1987).
18. H. H. Krbecek and M. Pietralla, J. Polym. Mater. 22, 177 (1993).
19. P. D. Davidse, H. Waterman, and J. B. Westerdijk, J. Polym. Sci. 59, 389–400 (1962).
20. B. Hartmann and J. Jarzynski, J. Polym. Sci. Part A-2, 9, 763–765 (1971).
21. R. K. Eby, J. Acoust. Soc. Am. 36, 1485–1487 (1964).
22. B. Hartmann, G. F. Lee, and J. D. Lee, J. Acoust. Soc. Am. 95, 226–233 (1994).
23. S. Havriliak and S. Negarni, J. Polym. Sci. Part C, No. 14, ed. R. F. Boyer (Interscience, New York, 1966), pp. 99–117.
24. I. I. Pavlinov, I. B. Rabinovich, V. Z. Pogorelko, and A. V. Ryabov, Polym. Sci. USSR AIO, 1471–1480 (1968).
25. B. Hartmann, J. Appl. Polym. Sci. 19, 3241–3255 (1975).
26. B. Hartmann and J. Jarzynski, J. Acoust. Soc. Am. 56, 1469–1477 (1974).
27. K. Shimizu, O. Yano, Y. Wada, and Y. Kawamura, J. Polym. Sci.: Phys. 11, 1641–1652 (1973).
28. N. Lagakos, J. Jarzynski, J. H. Cole, and J. A. Bucaro, J. Appl. Phys. 59, 4017–4031 (1986).
29. D. W. Phillips, A. M. North, and R. A. Pethrick, J. Appl. Polym. Sci. 21, 1859–1867 (1977).
30. B. Hartmann, J. Appl. Phys. 51, 310–314 (1980).
31. E. Morita, R. Kono, and H. Yoshizaki, Jpn. J. Appl. Phys. 7, 451–461 (1968).
32. H. Singh and A. W. Nolle, J. Appl. Phys. 30, 337–341 (1959).
33. I. I. Perepechko and V. E. Sorokin, Sov. Phys. Acoust. 18, 485–489 (1973).
34. B. Hartmann and G. Lee, J. Polym. Sci.: Phys. Ed. 20, 1269–1278 (1982).
35. E. Montgomery, F. J. Weber, D. F. White, and C. M. Thompson, J. Acoust. Soc. Am. 71, 735–741 (1982).
36. J. Sutherland, J. Appl. Phys. 49, 3941–3945 (1978).
37. B. Hartmann, Polymer 22, 736–739 (1981).
38. H. J. Sutherland and R. Lingle, J. Appl. Phys. 43, 4022–4026 (1972).
39. C. M. Thompson and W. L. Heimer, II, J. Acoust. Soc. Am. 77, 1229–1238 (1985).
40. N. V. Karyakin, I. B. Rabinovich, and V. A. Ulyanov, Polym. Sci. USSR 11, 3159–3164 (1969).
41. Y. Wada and K. Yamamoto, J. Phys. Soc. Jpn 11, 887–892 (1956).
42. B. Hartmann and J. Jarzynski, J. Appl. Phys. 43, 4304–4312 (1972).
43. B. Hartmann, "Ultrasonic Measurements", in *Methods of Experimental Physics,* Vol. 16c, ed. R. A. Fava, (Academic Press, New York, 1980), pp. 59–90.
44. D. L. Lamberson, J. R. Asay, and A. H. Guenther, "Polystyrene and Polymethylmethacrylate from Ultrasonic Measurements at Moderate Pressures", J. Appl. Phys. 43, 976–985 (1972).
45. J. R. Asay, D. L. Lamberson, and A. H. Guenther, J. Appl. Phys. 40, 1768–1783 (1969).
46. A. Lukashov, V. Feofanov, J. D. Schultze, M. Boehning, and J. Springer, Polymer 33, 2227–2228 (1992).
47. S. de Petris, V. Frosini, E. Butta, and M. Baccaredda, Makromol. Chemie. 109, 54–61, (1967).
48. I. I. Perepechko and V. A. Grechishkin, Polym. Sci. USSR A15, 1139–1148 (1973).
49. 13. Hartmann and G. F. Lee, J. Non-Cryst. Solids 131–133, 887–890 (1991).
50. J. V. Duffy, G. F. Lee, J. D. Lee, and B. Hartmann, in *Sound and Vibration Damping with Polymers,* eds. R. D. Corsaro and L. H. Sperling, ACS Symposium Series 424 (ACS Press, Washington, DC, 1990), pp. 281–300.
51. B. Hartmann, J. V. Duffy, G. F. Lee, and E. Balizer, J. Appl. Polym. Sci. 35, 1829–1852 (1988).
52. J.E. Carlson, J. van Deveneter, A. Scolan and C. Carlander, 2003 IEEE Ultrasonics Symposium, Honolulu, 5–8 Oct 2003, eds. D.E. Yuhas, and S.C. Schneider, IEEE, Piscataway, NJ, USA, pp. 885–888.
53. K. Matsushige, in *High Performance Polymers* (Hanser, New York, 1991), pp. 103–131.
54. H. Y. Guney, T. Oskay and H. S. Ozkan, J. Polym. Sci. B: Polym. Phys. 33, 985–991, (1995).
55. K.J. Suslick and G.J. Price, Annu. Rev. Mater. Sci. 29, 295–326, (1999).
56. I. Alig and D. Lellinger, Chem. Innovat. 30, 12–18, (2000).
57. D. Buckley, unpublished data.

CHAPTER 61

Permeability of Polymers to Gases and Vapors

S. A. Stern* and J. R. Fried†

*Department of Biomedical and Chemical Engineering, Syracuse University, Syracuse, NY 13244
†Department of Chemical and Materials Engineering, University of Cincinnati, Cincinnati, OH 45221

61.1 INTRODUCTION

All polymers are permeable to gases and vapors to different extents. Permeability is a physical property of great importance in a variety of industrial and biomedical applications of polymers. Examples of these applications include: the separation of gas and liquid mixtures, water desalination, food packaging, protective coatings (e.g., paints and varnishes), controlled drug release, and biomedical devices. Polymers are commonly used in these applications in the form of *nonporous* membranes (e.g., films or sheets, hollow fibers, or capillaries). The following discussion and accompanying references are based largely on studies made with such membranes. A *vapor* is defined in this chapter as a gas at a temperature below its critical temperature, i.e., as a condensable gas. Consequently, the term ''gas'' is used hereafter to designate both supercritical gases and vapors.

A large number of polymers have been synthesized for various applications that depend on gas permeability, but in particular for potential uses as membrane materials for gas separation processes. The permeability of these polymers to various gases has been measured at different temperatures and in some cases over a range of pressures. The objective of this chapter is to complement and update the compilations of gas permeability data already published in Chapter 50 of the first edition of this Handbook. Since, due to limitations of space, it was not possible to list gas permeability data at all the various temperatures and pressures at which these data have been determined, and since different readers have different interests, only references to permeability data have been given. However, all the gases used and the temperatures and pressures at which the referenced permeability measurements were made are listed. The references to gas permeabilities reported in this chapter are not comprehensive, but are representative of selected classes of homopolymers. References to some earlier gas permeability studies are included. This chapter also includes a brief review of the permeation mechanisms as well as a mention of the use of computer simulations of gas permeation in and through nonporous polymer membranes.

61.2 MECHANISMS OF GAS PERMEATION

61.2.1 Basic Relations and Definitions

Gases permeate through polymer membranes when a pressure differential is established at opposite membrane interfaces. The permeation of gases through *nonporous* polymer membranes is generally described in terms of a ''solution-diffusion'' mechanism [1–9]. According to this mechanism, gas permeation is a complex process consisting of the following sequence of events: (1) solution (absorption) of the gas into the membrane at its interface exposed to the higher pressure; (2) molecular (''random walk'') diffusion of the gas in and through the membrane; and (3) release of the gas from solution (desorption) at the opposite interface exposed to a lower pressure. The term *permeation* is accordingly used here to describe the overall mass transport of the penetrant gas across the membrane, whereas the term *diffusion* refers only to the movement of the penetrant molecules inside the polymer matrix.

In most practical applications, molecular diffusion is the slowest and, hence, the rate-determining step in the permeation process. By comparison, the absorption and desorption steps are very fast, so that solution equilibrium is assumed to be established between the gas phase in contact with the two membrane interfaces and the gas dissolved at these interfaces.

The diffusion of gas molecules in and through polymer membranes can in many cases of practical interest be described by Fick's two laws. Thus, for isothermal diffusion of a gas through a ν-dimensional hyperspherical membrane of sufficiently large area ($\nu = 1$ for a planar membrane or slab, $\nu = 2$ for a hollow cylinder, and $\nu = 3$ for a spherical shell), these laws are described by the following equations [1]:

$$J = -\omega_\nu r^{\nu-1} D(c) \frac{\partial c(r,t)}{\partial r} \tag{61.1}$$

and

$$\frac{\partial c}{\partial t} = \frac{1}{r^{\nu-1}} \frac{\partial}{\partial r} \left[r^{\nu-1} D(c) \frac{\partial c}{\partial r} \right] \quad R_1 < r < R_2, \tag{61.2}$$

where J is the local rate of penetrant gas diffusion (the local flux); $c(r,t)$ is the local penetrant concentration at a position coordinate r and at time t; $D(c)$ is the local mutual diffusion coefficient; $\omega_1 = 1$ for a planar membrane or slab; $\omega_2 = 2\pi$ for a hollow cylinder; and $\omega_3 = 4\pi$ for a spherical shell. The flux, J, is taken through unit area of slab, unit length of cylinder, and the whole area of the spherical shell. The diffusion coefficient, D, depends on temperature and the nature of the penetrant/polymer system and can be constant or a function of penetrant concentration.

Integration of Eq. (61.1) for the desired geometry and boundary conditions yields the total rate of permeation of the penetrant gas through the polymer membrane. Integration of Eq. (61.2) yields information on the temporal evolution of the penetrant concentration profile in the polymer. Equation (61.2) requires the specification of the initial and boundary conditions of interest. The above relations apply to homogeneous and isotropic polymers. Crank [3] has described various techniques of solving Fick's equations for different membrane geometries and boundary conditions, for constant and variable diffusion coefficients, and for both transient and steady-state transport.

The equilibrium concentration (solubility), c, of a penetrant gas dissolved in a polymer can be related to the pressure, p, of the penetrant by the isothermal relation

$$c = S(c) \cdot p, \tag{61.3}$$

where $S(c)$ [or $S(p)$] is a solubility coefficient. When the concentration of the penetrant in the polymer is very low, Eq. (61.3) reduces to a form of Henry's law; the solubility coefficient is then independent of c (or p). In the case of gas permeation Eq. (61.3) is applicable to the conditions prevailing at the membrane interfaces.

In practical applications it is often of interest to determine the rate of gas permeation under steady-state conditions. Steady state is achieved if, at a given temperature, the constant pressures p_h and $p_l (< p_h)$ are maintained at opposing membrane interfaces, respectively. For example, the following relation can be derived from Fick's first law, cf. Eq. (61.1), for the steady-state rate of gas permeation J_s through unit area of a planar, isotropic, and homogeneous membrane of effective thickness δ, i.e., when $\nu = 1$ and $\omega = 1$:

$$J_s = \overline{P}(p_h - p_l)/\delta, \tag{61.4}$$

where $\overline{P}$ is a mean "permeability coefficient" or "permeability"; Eq. (61.4) refers to a specified temperature and unit area of membrane. The ratio $\overline{P}/\delta$ is a mass-transfer coefficient.

Similarly, the steady-state rate of gas permeation through a tubular membrane, such as a capillary or hollow fiber, is given by the relation

$$J_s = \overline{P} \frac{2\pi L(p_h - p_l)}{\ln(R_o - R_i)}, \tag{61.5}$$

where R_o and R_i are the effective outer and inner radii of the tube, respectively, and L is the length of the tube. The mean permeability coefficient, $\overline{P}$, depends on the nature of the penetrant gas and polymer membrane, on the temperature, and, in the most general case, on both p_h and p_l. The rate of gas permeation of a component of a gas mixture is also given by Eqs. (61.4) and (61.5), but p_h and p_l are then the *partial* pressures of that component at opposite membrane interfaces and $\overline{P}$ may also be a function of composition.

61.2.2 Relations between Permeability, Diffusion, and Solubility Coefficients

It can be shown that the mean permeability coefficient $\overline{P}$ is a product of a mean diffusion coefficient, $\overline{D}$, and a function $\overline{S}$ related to the solubility of the penetrant gas in the polymer [1–9]:

$$\overline{P} \equiv \overline{D} \cdot \overline{S}, \tag{61.6}$$

where $\overline{D}$ is a mean diffusion coefficient

$$\overline{D} = \int_{c_l}^{c_h} [D(c)/(c_h - c_l)] dc \tag{61.7}$$

and $\overline{S}$ is a function defined by the relation

$$\overline{S} = \frac{(c_h - c_l)}{(p_h - p_l)}, \tag{61.8}$$

where c_h and $c_l (< c_h)$ are the equilibrium concentrations of the penetrant dissolved at the membrane interfaces at pressures p_h and p_l, respectively. When $p_h \gg p_l$, and therefore $c_h \gg c_l$ as is often the case, $\overline{S}$ reduces to

$$\overline{S} = S_h = c/p|_h, \tag{61.9}$$

where S_h is the solubility coefficient evaluated at the "upstream" pressure p_h, cf. Eq. (61.3).

When the solubility of a penetrant gas in a polymer is sufficiently low to be within the Henry's law limit, then $S(c) = S_o$, a constant at a given temperature, cf. Eq. (61.3). The mutual diffusion coefficient is then often also a constant, $D(c) = D_o$; this is the case for supercritical gases in "rubbery" polymers over wide ranges of pressure. Equation (61.6) then reduces to

$$P_o = D_o \cdot S_o, \tag{61.10}$$

where P_o depends only on the nature of the penetrant/polymer system and the temperature. This relation has been widely used in the literature, sometimes without qualification and sufficient justification. Equation (61.10) shows that P_o is a product of a diffusion coefficient, D_o (a kinetic factor), and of a solubility coefficient, S_o (a thermodynamic factor).

The problem of gas diffusion in, and permeation through, *inhomogeneous* polymers is more complex, but has been considered by a number of investigators [3,5,6,10]. The diffusion coefficient is then also a function of position. When the polymer is highly plasticized (i.e., swelled) by the penetrant, the diffusion coefficient may also become a function of time and of sample "history." Such "non-Fickian" diffusion has also been studied [3,5,11–16].

61.2.3 Gas Selectivity of Polymers

The overall *selectivity* of a polymer membrane toward two different penetrant gases A and B is commonly expressed in terms of an "ideal" separation factor, $\alpha^*(A/B)$, which is defined by the relation, cf., Eq. (61.6)

$$\alpha^*(A/B) \equiv \frac{\overline{P}(A)}{\overline{P}(B)} = \frac{\overline{D}(A)}{\overline{D}(B)} \cdot \frac{\overline{S}(A)}{\overline{S}(B)}, \tag{61.11}$$

where the ratios $\bar{D}(A)/\bar{D}(B)$ and $\bar{S}(A)/\bar{S}(B)$ are known, respectively, as the "diffusivity (or mobility) selectivity" and the "solubility selectivity." These ratios represent contributions to the overall selectivity due to the differences in the diffusivities and solubilities of gases A and B in a polymer.

61.2.4 Dependence on Temperature

In cases where the permeability coefficient for a gas/polymer system is independent of pressure, i.e., $\overline{P} = P_o$, the temperature dependence of P_o can be represented over small ranges of temperature by the Arrhenius-type relation

$$P_o = P_o^o \exp(-E_p/RT), \tag{61.12}$$

where P_o^o is a constant; E_p is the apparent energy of activation of the permeation process, R is the universal gas constant, and T is the absolute temperature. As mentioned above, P_o is independent of pressure when the mutual diffusion coefficient, D_o, is a constant (at constant temperature) and the solubility is within the Henry's law limit, i.e., the solubility coefficient, S_o, is a constant, cf., Eq. (61.10). In such cases, the temperature dependence of D_o can also be represented by the Arrhenius-type relation

$$D_o = D_o^o \exp(-E_d/RT), \tag{61.13}$$

whereas the temperature dependence of S_o is expressed by the van't Hoff-type relation

$$S_o = S_o^o \exp(-\Delta H_s/RT). \tag{61.14}$$

In equations (61.13) and (61.14) D_o^o and S_o^o are constants, E_d is an apparent activation energy of diffusion, and ΔH_s is the molar heat (enthalpy) of solution.

Equations (61.10), (61.12), (61.13), and (61.14) yield the following relations:

$$P_o^o = D_o^o \cdot S_o^o \tag{61.15}$$

and

$$E_p = E_d + \Delta H_s. \tag{61.16}$$

It follows from Eq. (61.16) that the sign and magnitude of E_p depend on the signs and relative values of E_d and ΔH_s. Since the value of E_d is always positive, D_o always increases with increasing temperature; ΔH_s can be either positive or negative, depending on the nature of the penetrant/polymer system, for the following reasons. The solution of a gas in a polymer can be visualized as occurring in two stages [1], namely, condensation of the gas to a liquid, followed by the mixing of the condensed gas with the polymer, i.e., solution in the polymer. Hence, the heat of solution, ΔH_s, can be expressed by the relation

$$\Delta H_s = \Delta H_{cond} + \Delta \bar{H}_1, \tag{61.17}$$

where ΔH_{cond} is the molar heat of condensation of the penetrant gas and $\Delta \bar{H}_1$ is the partial molar heat of mixing of the condensed gas with the polymer.

The molar heat of condensation, ΔH_{cond}, is a hypothetical quantity for supercritical gases, such as the helium-group gases, H_2, O_2, N_2, etc., at ambient temperature. It is assumed that ΔH_{cond} for such gases is very small. The value of ΔH_s then depends largely on that of $\Delta \bar{H}_1$, which is small and positive (i.e., the mixing process is endothermic). Therefore, ΔH_s for supercritical gases is commonly also small and positive, and the solubility coefficients S_o increases slightly as the temperature is raised, cf., Eq. (61.14). Equations (61.12) and (61.16) show that the permeability coefficient, P_o, then also increases with increasing temperature.

By contrast, for subcritical gases (vapors) ΔH_{cond} is the predominant term in Eq. (61.17). Since condensation is an exothermic process, ΔH_{cond} is negative. Therefore, the heat of solution, ΔH_s, of subcritical gases, such as organic vapors, is also negative and their solubility in polymers decreases with increasing temperature. In such cases, E_p may be either positive or negative depending on the relative values of E_d (which is always positive) and ΔH_s. Hence,

P_o for subcritical gases may increase, decrease, or change very little as the temperature is raised.

According to Eqs. (61.12), (61.13), and (61.14), plots of $\ln P_o$, $\ln D_o$, and $\ln S_o$ versus the reciprocal absolute temperature, $1/T$, should be linear over limited ranges of temperature in which E_p, E_d, and ΔH_s are constant. This is found to be the case for supercritical gases that exhibit a low solubility in polymers even at elevated pressures, provided that the polymers are not significantly plasticized (swelled) by the penetrant gases. The same linear plots are obtained with subcritical gases (which are more highly soluble in polymers) at very low penetrant gas concentrations, e.g., in the Henry's law limit. The plots of $\ln P_o$, $\ln D_o$, and $\ln S_o$ versus $1/T$ for different gases in rubbery and glassy polymers may exhibit single or double discontinuities (breaks), or no discontinuities at all, at or near the glass-transition temperature, T_g, of the polymers.

Equations (61.12), (61.13), and (61.14) can be applied over wider ranges of temperature if the dependence of E_p, E_d, and ΔH_s on temperature is known. For example, if E_p and E_d decrease with increasing temperature, plots of $\ln P_o$ and $\ln D_o$ versus $1/T$ are then curves with decreasing slopes.

When the permeability, diffusion, and solubility coefficients are functions of pressure their experimental values are mean values ($\overline{P}, \overline{D}$, and $\overline{S}$) for the pressures applied at the membrane interfaces, cf., eqs. (61.6–61.8). Equations (61.12–61.14) are applicable also to $\overline{P}, \overline{D}$, and $\overline{S}$ over a limited range of temperatures. The activation energies E_p and E_d commonly decrease with increasing pressure.

61.2.5 Dependence on Gas Pressure

The dependence of permeability, diffusion, and solubility coefficients on penetrant gas pressure (or concentration in polymers) is very different at temperatures above and below the glass transition temperature, T_g, of the polymers, i.e., for "rubbery" and "glassy" polymers, respectively. Thus, when the polymers are in the *rubbery* state the pressure dependence of these coefficients depends, in turn, on the gas solubility in polymers. For example, as mentioned in Section 61.2.4, if the penetrant gases are very sparsely soluble and do not significantly plasticize the polymers, the permeability coefficients as well as the diffusion and solubility coefficients are independent of penetrant pressure. This is the case for supercritical gases with very low critical temperatures (compared to ambient temperature), such as the helium-group gases, H_2, O_2, N_2, CH_4, etc., whose concentration in rubbery polymers is within the Henry's law limit even at elevated pressures.

Subcritical gases, such as organic vapors, are much more highly soluble in polymers, and, consequently, the above behavior is observed only at very low pressures (or concentrations in polymers). As the penetrant pressure is raised, and the polymers are increasingly plasticized by the penetrant gas, the permeability, diffusion, and solubility coefficients increase rapidly, in some cases exponentially, with increasing pressure.

By contrast, the permeability, diffusion, and solubility coefficients for gases in *glassy* polymers are strongly nonlinear functions of the penetrant gas pressure. Such a nonlinear behavior is observed even when the polymer is not significantly plasticized by the penetrant gas. This behavior is described satisfactorily by the "dual-mode" sorption model [3–7,9,17], which attributes it to the heterogeneity of glassy polymers. According to this model, the permeability and solubility coefficients decrease and the diffusion coefficients increase as the gas pressure is raised; all three coefficients reach asymptotic values at sufficiently high pressures. The dual-mode sorption model also shows that the permeability, diffusion, and solubility coefficients must become independent of pressure at sufficiently low pressures. Dual-mode sorption behavior has been observed experimentally with a variety of gases in many glassy polymers.

When the concentration of penetrant gases in glassy polymers becomes sufficiently high to plasticize the polymers, the permeability, diffusion, and solubility coefficients will deviate from dual-mode sorption behavior and increase as the pressure is raised.

61.2.6 Molecular Mechanisms and Computer Simulations

It has been shown in a previous section that, in most cases of practical interest, the rate of gas permeation through nonporous polymer membranes is controlled by the diffusion of the penetrant gas in the polymer matrix. Many theoretical models have been proposed in the literature to describe the mechanisms of gas diffusion in polymers on a *molecular* level. Such models provide expressions for gas diffusion coefficients, and sometimes also for permeability coefficients, derived from free volume, statistical–mechanical, energetic, structural, or other considerations. The formulation of these coefficients is complicated by the fact that gas transport occurs by markedly different mechanisms in rubbery and glassy polymers.

As a result, the mechanisms of gas transport in polymers are still incompletely understood, particularly below T_g, when considered on a microscopic level. Therefore, almost all transport models proposed in the literature are phenomenological and contain one or more adjustable parameters that must be determined experimentally. Moreover, most of these models have been found to be applicable only to a limited number of gas/polymer systems.

Clearly, a better understanding of the gas transport mechanisms in polymers would greatly facilitate the development of polymer membranes that exhibit both a higher selectivity and a higher (or lower) permeability to specified gases. It is beyond the scope of the present chapter to review this area of research, particularly since a number of extensive reviews are available [1,3–9,11–15,17,18].

It must be noted, however, that the development of very fast computers and recent advances in the computer simulation of polymer microstructures will make possible the formulation of much more realistic molecular models of gas transport in and through polymers. Information concerning self-diffusion and solubility, fractional free volume, *d*-spacing, and chain and substituent group mobility now can be obtained with good confidence by a variety of methods including molecular dynamics and Monte Carlo simulations using extensively parameterized polymer force fields such as COMPASS [19,20]. Several excellent reviews are available [21–24]. Recent developments in the applications of nonequilibrium molecular dynamics and Grand Canonical Monte Carlo methods following the work of Heffelfinger and Thompson [25,26] have extended the application of simulation methods to investigate transport through nonporous ''dense'' membrane as well as through membrane pores under a concentration gradient.

61.3 GAS PERMEABILITY DATA

A very large body of data on the gas permeability of many rubbery and glassy polymers has been published in the literature. These data were obtained with homopolymers as well as with copolymers and polymer blends in the form of nonporous ''dense'' (homogeneous) membranes and, to a much lesser extent, with asymmetric or ''composite'' membranes. The results of gas permeability measurements are commonly reported for ''dense'' membranes as permeability coefficients, and for asymmetric or composite membranes as ''permeances'' (permeability coefficients not normalized for the effective membrane thickness). Most permeability data have been obtained with pure gases, but information on the permeability of polymer membranes to a variety of gas mixtures has also become available in recent years. Many of the earlier gas permeability measurements were made at ambient temperature and at atmospheric pressure. In recent years, however, permeability coefficients as well as solubility and diffusion coefficients for many gas/polymer systems have been determined also at different temperatures and at elevated pressures. Values of permeability coefficients for selected gases and polymers, usually at a single temperature and pressure, have been published in a number of compilations and review articles [27–35].

It should be noted that the gas and vapor permeability of polymer membranes could be affected by pretreatment, ageing, plasticization, crosslinking and/or crystallinity of the polymer and, in some cases, by the experimental conditions and measurement techniques employed. For example, the type of solvent(s) used in the casting of membranes may affect their permeability.

Tables 61.2–61.17 list references to many recent and some earlier permeability measurements made with various pure gases and membranes cast from different classes of rubbery and glassy polymers, but mainly homopolymers. The ranges of experimental pressure and temperature reported in these references are also listed. Values of permeability coefficients for some gas/polymer systems can also been obtained from a number of correlations mostly based on group contribution methods [36–41].

The permeability of different polymers to a given gas can vary by many orders of magnitude. The permeability of a given polymer to different gases, i.e., its gas selectivity, can also vary significantly. Glassy polymers commonly exhibit a low permeability but high gas selectivity. By contrast, rubbery polymers exhibit a higher permeability but a much lower selectivity than glassy polymers under comparable conditions. Glassy polymers are commonly much more permeable to light gases, such as He, H_2, N_2, O_2, and CO_2 than to organic vapors whereas the opposite is true for rubbery polymers. The separation of gases by selective permeation through rubbery polymer membranes is due mainly to differences in the gas solubility whereas separation by glassy polymer membranes is caused mainly by differences in the gas diffusivity.

Some exceptions to the above behavior are known, such as in the case of poly(1-trimethylsilyl-1-propyne), PTMSP, a glassy polymer at ambient temperature. PTMSP has the highest gas permeability of all known synthetic polymers but a low gas selectivity due to its very large free volume. Although in the glassy state, this polymer is more permeable to organic vapors than to light gases.

The permeability coefficients of gases in rubbery polymers can also be used in calculations involving gas mixtures if the gas solubility in the polymers is sufficiently low, e.g., in the Henry's law limit. This is due to the fact that under such conditions the components of gas mixtures commonly permeate through a polymer membrane independently of each other. By contrast, the permeation of the components of gas mixtures in and through glassy polymers is ''coupled,'' i.e., each component affects the permeation behavior of the other component(s). Commonly, the permeation rate of the ''faster'' component(s) of a gas mixture is decreased while that of the ''slower'' component(s) is increased, thus decreasing the polymer selectivity. This behavior is quantitatively described by the ''dual-mode sorption'' model and its extensions [5–9,12,17].

The following tables also list values of T_g in order to facilitate the identification of polymers with high or low gas permeabilities and high or low gas selectivities. The T_gs were either stated in the listed references or, in some cases, obtained from other sources; values of T_g reported by different investigators for a given polymer sometimes may differ by 10 °C or more, depending on the method and time frame of the measurements and on other factors.

61.4 GAS PERMEABILITY UNITS

The permeability coefficient $\overline{P}$ for pure gases is defined by Eq. (61.4) in the form

$$\overline{P} = \frac{J_s \cdot \delta}{(p_h - p_l)}$$

where J_s is the *mass* of penetrant gas permeating per unit time through unit area of a membrane of effective thickness δ under a pressure differential $(p_h - p_l)$. Consequently, $\overline{P}$ has the following dimensions:

$$\overline{P}\left[\frac{\text{(mass of permeating gas)(effective membrane thickness)}}{\text{(time)(membrane area)(pressure difference across membrane)}}\right].$$

The effective thickness of ''asymmetric'' or ''composite'' membranes is much smaller than their actual thickness [6,9] and may not be known. Therefore, the permeability to gases of such membranes is often characterized by their ''permeance,'' $\overline{P}/\delta$.

A variety of units for $\overline{P}$ have been used by different investigators. Some of these units and their conversion factors are listed in Table 61.1.

The standard temperature and pressure (STP) are, respectively, 273.15 K and 1 atm. $(1.013 \times 10^5\,\text{Pa})$; $1\text{mil} = 1 \times 10^{-3}$ in. $= 2.540 \times 10^{-3}$cm; $1\text{in.}^2 = 6.4516\,\text{cm}^2$. The unit [in.^{3}(STP)·mil/(day·100 in.^{2} atm.)] has been used mainly in packaging applications. The quantity 1×10^{-10} $\left[\frac{\text{cm}^3\text{(STP)}\cdot\text{cm}}{\text{s}\cdot\text{cm}^2\cdot\text{cmHg}}\right]$ is designated by some investigators as ''1 Barrer''.

ACKNOWLEDGMENTS

This chapter is a revised and updated version of Chapter 50, ''Permeability of Polymers to Gases and Vapors'' by S. A. Stern, B. Krishnakumar, and S. M. Nadakatii, published in the first edition of ''Physical Properties of Polymers Handbook'', J. E. Mark, Editor, AIP Press, Woodbury, NY, 1996, pp. 687–700.

TABLE 61.1. *Various units of $\overline{p}$ used by different investigators.*

Unit	Multiplication factor		
	$\frac{\text{cm}^3\text{(STP)}\cdot\text{cm}}{\text{s}\cdot\text{cm}^2\cdot\text{cmHg}}$	$\frac{\text{cm}^3\text{(STP)}\cdot\text{cm}}{\text{s}\cdot\text{cm}^2\cdot\text{Pa}}$	$\frac{\text{in}^3\text{(STP)}\cdot\text{mil}}{\text{day}\cdot 100\,\text{in.}^2\cdot\text{atm.}}$
$\frac{\text{cm}^3\text{(STP)}\cdot\text{cm}}{\text{s}\cdot\text{cm}^2\cdot\text{cmHg}}$	1	7.5×10^{-4}	1.02×10^{11}
$\frac{\text{cm}^3\text{(STP)}\cdot\text{cm}}{\text{s}\cdot\text{cm}^2\cdot\text{Pa}}$	1.33×10^{3}	1	1.36×10^{14}
$\frac{\text{in}^3\text{(STP)}\cdot\text{mil}}{\text{day}\cdot 100\,\text{in.}^2\cdot\text{atm.}}$	9.82×10^{-12}	7.37×10^{-15}	1

TABLE 61.2. *Polyolefins.*

Polymer	Gases and vapors	T_g(°C)	Temperature (°C)	Pressure (atm.)	Ref.
Polyethylene	He, Ar, N_2, O_2, CO, CO_2, CH_4, C_2H_6, C_3H_4, C_3H_6, C_3H_8, SF_6	−20[a]	5–55	NR	[42]
	Ar, CF_4, $C_2H_2F_2$, SF_6	NR	5–50	1–15	[43]
	He, N_2, CO_2, CH_4, C_2H_4, C_2H_6, N_2O	NR	−10 to 60	1–60	[44]
	N_2, O_2, CO_2	NR	30	≤1	[45]
	He, Ne, Ar, Kr, H_2, N_2, O_2, CO_2, CH_4, N_2O	NR	25	1–130	[46]
	He, CO_2, CH_4	NR	35	1	[47]
Polyisobutene	He, H_2, N_2, O_2, CO_2, CH_4	−76[a]	17–50	1	[48]
Poly(4-methyl pentene-1)	N_2, O_2	29[a]	25	1.36	[49]
Polypropylene	He, Ne, Ar, Kr, H_2, N_2, O_2, CO_2, CH_4, N_2O	−1 to −13[a]	25	1–130	[46]
	O_2	NR	NR	NR	[50]

NR, not reported in cited reference.
[a]Value of T_g not from cited reference.

TABLE 61.3. *Vinyl and vinylidene polymers.*

Polymer	Gases and vapors	T_g (°C)	Temperature (°C)	Pressure (atm.)	Ref.
Poly(vinyl chloride)	CO_2	76	40–55	≤1	[51]
	He, Ne, Ar, Kr, H_2, N_2, O_2, CO_2, CH_4, H_2O	75	25	NR	[52]
Poly(vinyl alcohol)	O_2	85[a]	25	NR	[53]
	O_2, H_2O	NR	25	NR	[54]
Poly(vinyl acetate)	Ar, CO_2	32	8–45	≤1	[55]
Polystyrene	CO_2	NR	35	1–23	[56]
	CO_2	98	25–40	≤1	[51]
	CH_4, C_3H_8, *n*-C_4H_10, *iso*-C_4H_10	101	25–50	NR	[57]
	He, H_2, N_2, O_2, CO_2	NR	25	NR	[58]
	N_2, O_2, CO_2, H_2O	NR	25–30	NR	[59]
Poly(vinylidene chloride)	O_2	−18	35	NR	[60]
	N_2, O_2, CO_2, H_2O	NR	25–30	NR	[59]
	H_2O	NR	25	NR	[61]
	N_2, O_2, CO_2	NR	30	≤1	[45]
Poly(vinylidene fluoride)	He, CO_2, CH_4	−40[a]	35	1	[47]
Poly(vinyl benzoate)	He, N_2, CO_2, CH_4	74[a]	20–80	0.1–100	[62]

NR, not reported in cited reference.
[a]Value of T_g not from cited reference.

TABLE 61.4. *Natural and synthetic rubbers.*

Polymer	Gases and vapors	T_g(°C)	Temperature (°C)	Pressure (atm.)	Ref.
1,4-Polybutadiene	Ne, H_2, N_2, CO_2	−7[a]	15–65	NR	[63]
	H_2, N_2, O_2, CO_2, CH_4	NR	17–50	1	[48]
Poly(dimethyl butadiene)	He, H_2, N_2, O_2, CO_2, CH_4	−11[a]	17–50	1	[48]
cis-Polyisoprene	He, H_2, N_2, O_2, CO_2, CH_4	−73[a]	17–50	1	[48]
	Ar, N_2, O_2, CO, CO_2, CH_4, C_3H_6, C_3H_8, SF_6	NR	15–55	NR	[42]
trans-Polyisoprene	C_3H_8	−65	50	NR	[64]
	H_2	−58[a]	17	NR	[65]
Polychloroprene	He, H_2, N_2, O_2, CO_2, CH_4	NR	17–50	1	[48]

NR, not reported in cited reference.
[a]Value of T_g not from cited reference.

TABLE 61.5. *Polyesters and polycarbonates.*

Polymer	Gases and vapors	T_g(°C)	Temperature (°C)	Pressure (atm.)	Ref.
Poly(ethylene terephthalate)	CO_2	60–86[a]	25–115	2–20	[66]
	CO_2	69	25–40	≤1	[51]
	He, Ar, H_2, N_2, CO_2	NR	50	NR	[67]
Poly(ethylene terephthalate) (Mylar A™)	N_2, O_2, CO_2	NR	30	≤1	[45]
Bisphenol-A polycarbonate	CO_2	144[a]	35	1–20	[68]
	He, N_2, O_2, CO_2, CH_4	150	35	≤60	[69]
Bisphenol-A polyarylate	CO_2, CH_4	184	35	≤16	[70]
Tetramethylbisphenol-A PC[b]	He, N_2, O_2, CO_2, CH_4	193	35	≤60	[69]
Hexafluorobisphenol-A PC[b]	He, N_2, O_2, CO_2, CH_4	176	35	≤60	[69]
Tetramethylhexafluoro-bisphenol-A PC[b]	He, N_2, O_2, CO_2, CH_4	208	35	≤60	[69]

NR, not reported in cited reference.
[a]Value of T_g not from cited reference.
[b]PC, polycarbonate.

TABLE 61.6. *Cellulose and cellulose derivatives.*

Polymer	Gases and vapors	T_g(°C)	Temperature (°C)	Pressure (atm.)	Ref.
Cellulose	H_2, N_2, O_2, CO_2, SO_2, H_2S, NH_3	− 30 to 160[a]	25	NR	[71]
Cellulose acetate	Ar, Kr, Xe, N_2, O_2, CO_2	NR	−5 to 85	≤1	[72]
Cellulose acetate	N_2, O_2, CO_2	NR	30	≤ 1	[45]
Cellulose acetate	He, N_2, CO_2, CH_4	NR	20–80	≤ 100	[62]
Cellulose acetate (DS = 1.75)[b]	He, H_2, N_2, O_2, CO_2, CH_4	205–212	35	≤30	[73]
Cellulose acetate (DS = 2.45)[b]	He, H_2, N_2, O_2, CO_2, CH_4	187, 198	35	≤30	[73]
Cellulose acetate (DS = 2.84)[b]	He, H_2, N_2, O_2, CO_2, CH_4	185, 187	35	≤30	[73]
Cellulose nitrate	Ar, N_2, O_2, CO_2, SO_2	53[a], 66[a]	25	NR	[71]
Ethyl cellulose	N_2, O_2, CO_2	43[a]	30	≤1	[45]
Ethyl cellulose (DS = 2.3–2.4)[b]	He, N_2, O_2, CO_2, CH_4	113–115	35	4–13.6	[74]
Ethyl cellulose (DS = 2.41–2.51)[b]	He, N_2, O_2, CO_2, CH_4	113–115	35	4–13.6	[74]
Ethyl cellulose (DS = 2.55+)[b]	He, N_2, O_2, CO_2, CH_4	128–133	35	4–13.6	[74]
Trifluoroacetylated ethyl cellulose	N_2, O_2	≅ 135	20	1.58–2.37	[75]

NR, not reported in cited reference.
[a]Value of T_g not from cited reference.
[b]DS, degree of substitution.

TABLE 61.7. *Fluoropolymers.*

Polymer	Gases and vapors	T_g(°C)	Temperature (°C)	Pressure (atm.)	Ref.
Polytetrafluoroethylene	H_2, N_2, O_2, CO_2, NO_2, N_2O_4	−73[a]	25	1	[76]
Poly(tetrafluoroethylene-*co*-hexafluoropropylene) (Teflon-FEP)™	CH_4, C_2H_6, C_3H_8, C_4H_10	NR	90	NR	[77]
Poly(trifluorochloroethylene)	N_2, O_2, CO_2, CH_4, C_2H_4, C_2H_6, C_3H_8	NR	25	1	[78]
(Kel-F)™	N_2, O_2, CO_2, H_2O	NR	25–30	NR	[59]

NR, not reported in cited reference.
[a]Value of T_g not from cited reference.

TABLE 61.8. *Polyorganosiloxanes.*

Polymer	Gases and vapors	T_g(°C)	Temperature (°C)	Pressure (atm.)	Ref.
Polydimethylsiloxane	He, Ar, Ne, Kr, Xe,H_2, N_2, O_2, *n*-C_4H_10	−123[a]	−78 to 0	NR	[79]
	He, N_2, O_2, CO_2, CH_4, C_2H_4, C_2H_6, C_3H_8	−123	10–55	1–9	[80]
	N_2, O_2	−123	30	NR	[81]
	NH_3	−123	10–55	1–7.8	[82]
	H_2	−123	10–55	1–6.8	[83]
Poly(methylethylsiloxane)	He, N_2, O_2, CO_2, CH_4, C_2H_4, C_2H_6, C_3H_8	−135	10–55	1–9	[80]
	N_2, O_2	−135	30	NR	[81]
	NH_3	−135	10–55	1–7.8	[82]
	H_2	−135	10–55	1–6.8	[83]
Poly(methylpropylsiloxane)	He, N_2, O_2, CO_2, CH_4, C_2H_4, C_2H_6, C_3H_8	−120	10–55	1–9	[80]
	N_2, O_2	−120	30	NR	[81]
	NH_3	−120	10–55	1–7.8	[82]
	H_2	−120	10–55	1–6.8	[83]
Poly(methyloctylsiloxane)	He, N_2, O_2, CO_2, CH_4, C_2H_4, C_2H_6, C_3H_8	−92	10–55	1–9	[80]
	N_2, O_2	−92	30	NR	[81]
	NH_3	−92	10–55	1–7.8	[82]
	H_2	−92	10–55	1–6.8	[83]
Poly(trifluoropropylmethylsiloxane)	He, N_2, O_2, CO_2, CH_4, C_2H_4, C_2H_6, C_3H_8	−70	10–55	1–9	[80]
	N_2, O_2	−70	30	NR	[81]
	NH_3	−70	10–55	1–7.8	[82]
	H_2	−70	10–55	1–6.8	[83]

TABLE 61.8. *Continued.*

Polymer	Gases and vapors	T_g(°C)	Temperature (°C)	Pressure (atm.)	Ref.
Poly(phenylmethylsiloxane)	He, N_2, O_2, CO_2, CH_4, C_2H_4, C_2H_6, C_3H_8	−28	10–55	1–9	[80]
	N_2, O_2	−28	30	NR	[81]
	NH_3	−28	10–55	1–7.8	[82]
	H_2	−28	10–55	1–6.8	[83]
Poly(dimethylsilmethylene)	He, N_2, O_2, CO_2, CH_4, C_2H_4, C_2H_6, C_3H_8	−92	10–55	1–9	[80]
	N_2, O_2	−92	30	NR	[81]
	NH_3	−92	10–55	1–7.8	[82]
	H_2	−92	10–55	1–6.8	[83]
Poly(silethylenesiloxane)	He, N_2, O_2, CO_2, CH_4, C_2H_4, C_2H_6, C_3H_8	−88	10–55	1–9	[80]
	N_2, O_2	−88	30	NR	[81]
	NH_3	−88	10–55	1–7.8	[82]
	H_2	−88	10–55	1–6.8	[83]
Poly(silhexylenesiloxane)	He, N_2, O_2, CO_2, CH_4, C_2H_4, C_2H_6, C_3H_8	−90	10–55	1–9	[80]
	N_2, O_2	−90	30	NR	[81]
	NH_3	−90	10–55	1–7.8	[82]
	H_2	−90	10–55	1–6.8	[83]
Poly(siloctylenesiloxane)	He, N_2, O_2, CO_2, CH_4, C_2H_4, C_2H_6, C_3H_8	−88	10–55	1–9	[80]
	N_2, O_2	−88	30	NR	[81]
Poly(*m*-silphenylenesiloxane)	He, N_2, O_2, CO_2, CH_4, C_2H_4, C_2H_6, C_3H_8	−48	10–55	1–9	[80]
	N_2, O_2	−48	30	NR	[81]
	NH_3	−48	10–55	1–7.8	[82]
	H_2	−48	10–55	1–6.8	[83]
Poly(*p*-silphenylenesiloxane)	He, N_2, O_2, CO_2, CH_4, C_2H_4, C_3H_8	−18	10–55	1–9	[80]
	N_2, O_2	−18	30	NR	[81]
	NH_3	−18	10–55	1–7.8	[82]

NR, not reported in cited reference.
[a]Value of T_g not from cited reference.

TABLE 61.9. *Polynitriles.*

Polymer	Gases and vapors	T_g(°C)	Temperature (°C)	Pressure (atm.)	Ref.
Polyacrylonitrile	He, Ne, Ar, Kr, N_2, Kr, N_2, O_2,CO_2	95	25–135	NR	[84]
	CO_2	95	35–55	5–13	[85]
	H_2O	NR	15–45	0–0.8[b]	[86]
Polyacrylonitrile (Barex™)	O_2, CO_2, H_2O	NR	25–38	NR	[54]
Poly(methacrylonitrile)	O_2,H_2O	120[a]	25	NR	[53]
	O_2, CO_2, H_2O	NR	25–38	NR	[54]

NR, not reported in cited reference.
[a]Value of T_g not from cited reference.
[b]Relative vapor pressure.

TABLE 61.10. *Polyamides.*

Polymer	Gases and vapors	T_g (°C)	Temperature (°C)	Pressure (atm.)	Ref.
Nylon 6	N_2, O_2, CO_2	40[a]	0–90	NR	[87]
	N_2, O_2, CO_2, H_2O	NR	25–30	NR	[59]
	H_2S	NR	0–80	0.25–1	[88]
Nylon 6,6	H_2O	42 (at 0.0% RH)	25–45	30–90% RH	[89]
	CO_2	50[a]	25	NR	[90]
	H_2O	NR	10–100	10–90% RH	[61]
Nylon 11	He, Ne, Ar, H_2, N_2, CO_2	42–92[a]	≤60	0.04–0.2	[91]
Pendent phenyl-substituted aromatic polyamides	He, H_2, N_2, O_2, CO_2, CH_4	297–328	35	≤20	[92]

NR, not reported in cited reference.
[a]RH, relative humidity.
Value of T_g not from cited references.

TABLE 61.11. *Polyimides.*

Polymer	Gases and vapors	T_g (°C)	Temperature (°C)	Pressure (atm.)	Ref.
PMDA-ODA	N_2, O_2	410	25	NR	[93]
	CO_2	420	35–80	10–20	[94]
	He, N_2, O_2, CO_2, CH_4	NR	35	2–10	[95]
	CO_2	NR	60	2.7–16.3	[96]
	N_2, O_2	410	25–40	NR	[93]
PMDA-MDA	He, N_2, O_2, CO_2, CH_4	338	35	2–10	[95]
PMDA-IPDA	He, N_2, O_2, CO_2, CH_4	NR	35	2–10	[95]
PMDA-3-BDAF	H_2, N_2, O_2, CO_2, CH_4	235	35	2–9	[97]
PMDA-4-BDAF	H_2, N_2, O_2, CO_2, CH_4	310	35	2–9	[97]
BPDA-ODA	H_2, N_2, O_2, CO, CO_2, CH_4	270	35	2–10	[98]
	CO_2	270	80	2–28	[99]
	H_2, CO, CO_2, CH_4	270	50	10	[100]
	H_2, CO, CO_2, CH_4	270	50	10	[101]
BPDA-MDA	H_2, CO, CO_2, CH_4	300	35	10	[98]
	H_2, CO, CO_2, CH_4	300	≦120	10	[101]
BTDA-ODA	H_2, N_2, O_2, CO, CO_2, CH_4	266	35	2–10	[98]
BTDA-DATPA	H_2, N_2, O_2, CO, CO_2, CH_4	292	35	2–10	[98]
6FDA-*p*-ODA	H_2, N_2, CO_2, CH_4	299	25	1	[98]
	CO_2, CH_4	293	25	4.87	[102]
	H_2, N_2, O_2, CO_2, CH_4	288	35	2–9	[97]
6FDA-*m*-PDA	H_2, N_2, O_2, CO, CO_2, CH_4	298	35–80	2–10	[103]
	H_2, N_2, O_2, CO_2, CH_4	285	35	1.4–8.2	[104]
6FDA-*m*-ODA	H_2, N_2, O_2, CO_2, CH_4	244	35	2–9	[97]
6FDA-*p*-PDA	H_2, N_2, O_2, CO, CO_2, CH_4	351	35–80	2–10	[103]
	CO_2, CH_4	342	25	4.87	[102]
	H_2, N_2, O_2, CO_2, CH_4	305	35	2–9	[97]
6FDA-3,4′-ODA	CO_2, CH_4	248	25	4.87	[102]
6FDA-IPDA	CO_2, CH_4	298	25	4.87	[102]
6FDA-4-BDAF	H_2, N_2, O_2, CO_2, CH_4	262	35	2–9	[97]
6FDA-2,4-DATr	H_2, N_2, O_2, CO_2, CH_4	342	35	1–7	[104]
6FDA-2,6-DATr	H_2, N_2, O_2, CO_2, CH_4	372	35	1–7	[104]
6FDA-3,5-DBTF	H_2, N_2, O_2, CO_2, CH_4	284	35	1–7	[104]
6FDA-3-BDAF	H_2, N_2, O_2, CO_2, CH_4	224	35	2–9	[97]
6FDA-based polyimides	C_2H_4, C_2H_6, C_3H_6, C_3H_8	305–320	35	17	[105]
	C_3H_6, C_3H_8	217–406	25	1.12–10.3	[106]
	1,3-butadiene, *n*-butane	237–376	25	1.1–2	[107]
Indan-containing	H_2, N_2, O_2, CO_2	232–274	22.5	1.23	[108]
polyimides	N_2, O_2, CO_2, CH_4	NR	35	10	[109]
Aromatic polyimides	He, N_2, O_2, CO_2, CH_4	253–265	30	3	[110]
	H_2O	262–452	85–135	0.197–0.622	[111]
Aromatic polyimides (contains also references to other polyimides)	N_2, O_2	246–304	35	NR	[112]
6FDA-Durene polyimides	He, H_2, N_2, O_2, CO_2, CH_4	NR	35	2–10	[113]
Fluorinated 6FDA-based polyimides	C_3H_6	300–406	25	2–10	[114]
Polyimides with fluorinated side-groups	N_2, O_2, CO_2, CH_4	200–301	25	5	[115]
6FDA-based polyimide	He, N_2, O_2, CO_2, CH_4	NR	30–50	3.5–20	[116]
	C_2H_4, C_2H_6, C_3H_6, C_3H_8	NR	35	C_2's: 2.5–16 C_3's: 2.0–8.4	[117]
	N_2, O_2, CO_2, CH_4	336	30–50	3.5–20	[118]
	He, H_2, N_2, O_2, CO_2, CH_4	NR	35	10	[119]
Thianthrene-5,5,10,10-tetraoxide-containing polyimides	H_2, N_2, O_2, CO_2, CH_4	NR	35	2[a]	[120]
Hyperbranched polyimides	He, H_2, O_2, CO_2, CH_4	339[b]	35	1	[121]
Poly(amide imide)s	N_2, O_2, CO_2, CH_4	237–350	35–75	1–20	[122]
PMDA-, BPDA-, and DSDA-based polyimides	H_2O	NR	85	0.395	[123]
Poly(phenylene thioether imide)s	N_2, O_2, CO_2, CH_4	216–292	35	1–10	[124]

NR, not reported in cited reference.
[a] TADATO/DSDA (1/1)-DDBT; N_2, CO_2, CH_4: 1–10 atm.
[b] Uncrosslinked 6FDA-TAPA.

TABLE 61.12. *Polyurethanes.*

Polymer	Gases and vapors	T_g (°C)	Temperature (°C)	Pressure (atm.)	Ref.
Polyurethane	N_2, O_2	−22 to −64[a]	25	NR	[125]
	N_2, O_2	−0.7 to −64[a]	25	NR	[126]
Amine-containing polyurethane and poly(urethane urea)	He, H_2, N_2, O_2, CO_2, CH_4	−18 to 27	35	10	[127]

NR, not reported in cited reference.
[a]Value of T_g not from cited reference.

TABLE 61.13. *Polyoxides.*

Polymer	Gases and vapors	T_g (°C)	Temperature (°C)	Pressure (atm.)	Ref.
Poly(ethylene oxide)	He, H_2, N_2, O_2, CO_2, C_2H_4, C_2H_6, C_3H_6, C_3H_8	−50[a]	25–45	4.4–14.6	[128]
Poly(phenylene oxide)	CH_4, C_2H_4, C_2H_6	NR	25	4.93	[129]
	CO_2	NR	35	1–25	[56]
	N_2, O_2, CO_2, CH_4	214	35	1	[130]
Sulfonated poly(phenylene oxide)	H_2, N_2, O_2, CO_2	NR	23–24	6.58	[131]
2,6-Dimethyl-1,4-poly(phenylene oxide)	CO_2, CH_4	210	35	1–25	[132]
2,6-Dimethyl-1,4-poly(phenylene oxide) bromide (36% Br)	CO_2, CH_4	233	35	1–25	[132]
2,6-Dimethyl-1,4-poly(phenylene oxide) bromide (bromide-91%)	CO_2, CH_4	262	35	1–25	[132]

NR, not reported in cited reference.
[a]Value of T_g not from cited reference.

TABLE 61.14. *Polysulfones.*

Polymer	Gases and vapors	T_g (°C)	Temperature (°C)	Pressure (atm.)	Ref.
Polysulfone	H_2	190	40	4–27	[133]
	He, N_2, O_2, CO_2, CH_4	186	35	1–20	[134]
Bisphenol-A polysulfone	He, Ar, CO_2, CH_4	185	35	1–20	[135]
	CO_2, CH_4	186	35	1–14	[70]
Polyethersulfone	N_2, O_2, CO_2	225	30	≤30	[136]
Polyarylether sulfone	H_2, He, Ar, N_2, O_2, CO, CO_2, CH_4	260	25–160	NR	[137]
Tetramethyl bisphenol-A polysulfone	He, N_2, O_2, CO_2, CH_4	230	35	1–20	[134]
Polysulfone[a] and polysulfones with pendent groups	N_2, O_2, CO_2	188.1[a]	35	1	[138]
Polysulfones with trimethylsilyl groups	N_2, O_2	155–165	35	1	[139]
Silyl-modified polysulfones and poly(phenyl sulfones)	N_2, O_2, CO_2	149–280	35	1	[140]
	H_2, N_2, O_2, CO_2, CH_4	117–225	35	1	[141]

NR, not reported in cited reference.
[a]Value of T_g not from cited reference.

TABLE 61.15. *Polyacetylenes.*

Polymer	Gases and vapors	T_g (°C)	Temperature (°C)	Pressure (atm.)	Ref.
Poly(1-trimethylsilyl-1-propyne) (PTMSP)	H_2, Xe, N_2, O_2, H_2O, SF_6, N_2O, CH_3OH, CH_4, C_2H_2, C_2H_6, C_3H_8, *n*-C_4H_{10}, *i*-C_4H_{10}	230	22	0–1	[142]
	N_2, O_2, CO_2, CH_4	200	35	1–27	[143]
	N_2, O_2, CO_2, CH_4, H_2O, CH_2Cl_2, dimethylketone, toluene	NR	Gases: 20–70 Vapors: 40–65	Gases: 0.987 Vapor activity: 0.02–0.1	[144]
	H_2, N_2, O_2, CO_2, CH_4, C_2H_6, C_3H_8, CF_4, C_2F_6, C_3F_8	NR	35	2–17; $C_3H_8 \leq 4.5$; $C_3F_8 \leq 9$	[145]
	Ethylbenzene	NR	35–55	VP: 1.64–4.40 cmHg	[146]
Poly(1-trimethylgermyl-1-propyne) (PTMGP)	H_2, N_2, O_2, CO_2, CH_4, C_3H_8,*n*-C_4H_{10}	>250	35	4.4 *n*-C_4H_{10}: 1.7	[147]
Poly(*tert*-butylacetylene)	He, H_2, N_2, O_2, CO_2, CH_4	>200	25	1	[148]
Poly(1-chloro-2-phenylacetylene)	He, H_2, N_2, O_2, CO_2, CH_4	>200	25	1	[148]
Substituted polyacetylenes	He, N_2, O_2, CO_2, CH_4	NR	25	NR	[149]
Highly branched substituted polyacetylenes	He, H_2, N_2, O_2, CO_2, CH_4, C_2H_6, C_3H_8, n-C_4H_{10}	>270 to >430	35	4.4 *n*-C_4H_{10}: 1.7	[150]
Poly(diphenylacetylene)s	He, N_2, O_2, CO_2, CH_4	NR	25	NR	[66]
Poly[1-phenyl-2-[*p*-(triisopropylsilyl) phenyl acetylene]	He, H_2, N_2, O_2, CO_2, CH_4, C_2H_6, C_3H_8, n-C_4H_{10}	NR	35	4.4 *n*-C_4H_{10}: 1.7	[151]

NR, not reported in cited references
VP, vapor pressure.

TABLE 61.16. *Polyacrylics.*

Polymer	Gases and vapors	T_g (°C)	Temperature (°C)	Pressure (atm.)	Ref.
Poly(methyl methacrylate)	He, Ar, H_2, N_2, O_2, CO_2, CH_4	106	35	1	[152]
Poly(ethyl methacrylate)	He, Ne, Ar, Kr, N_2, O_2, CO_2, H_2S, H_2O	66[a]	25–85	NR	[153]
	Ar, N_2, O_2, CO_2, CH_4	69	35	0–35	[154]

NR, not reported in cited reference.
[a]Value of T_g not from cited reference.

TABLE 61.17. *Miscellaneous polymers.*

Polymer	Gases and vapors	T_g (°C)	Temperature (°C)	Pressure (atm.)	Ref.
Poly(ether ketone)s with indan groups in main chain	H_2, N_2, O_2, CO_2	218–255	22.5	1.23	[155]
Poly(3-dodecylthiophene)	N_2, O_2, CO_2	−20	35–37	1.45	[156]
Polyphosphazenes	H_2, N_2, O_2, CO_2, CH_4, C_2H_6, C_3H_8	−82 to −66	35	13.6 C_3H_8: 2.72	[157]
Poly(lactic acid)	He, H_2, N_2, O_2, CO_2, CH_4	−81 to 4	30	2.04	[158]
	N_2, O_2, CO_2, CH_4	58	30	2.63[a]	[159]
Polyarylates	H_2O	183–261	40	Vapor activity: 0–0.8	[160]
Poly(arylene ether)s	H_2, N_2, O_2, CO_2, CH_4	119–155	30–75	1	[161]
Poly(aryl ether ketone)s	He, N_2, O_2, CO_2, CH_4	175–203	30	3	[162]
Bis(phenyl)fluorene-based cardo polymers	N_2, CO_2	150–492	25	1	[163]
Cardo poly(arylether)s	H_2, N_2, O_2, CO_2, CH_4	218–289	30–100	NR	[164]
Oxyalkylenes with alkylsulfonylmethyl side chains	O_2	37–126	30	3.26	[165]

TABLE 61.17. *Continued.*

Polymer	Gases and vapors	T_g(°C)	Temperature (°C)	Pressure (atm.)	Ref.
Poly(arylene ether ketone)s	He, N_2, O_2, CO_2, CH_4	159–260	35	1.70–13.6	[166]
Polynorbornenes with aliphatic pendant groups	He, H_2, N_2, O_2, CO_2, CH_4	150–>380	35	10	[167]
ROMP polymers from silyl-substituted norbornadienes and norbornenes	He, H_2, N_2, O_2, CO_2, CH_4, C_2H_6	85–167	22	0.1–1	[168]
Alkyl-substituted poly(norbornene)	H_2O, Methanol	150–380	30	Vapor activity: 1	[169]
Polypyrrolones	He, N_2, O_2, CO_2, CH_4	NR	35–80	He, N_2, CO_2, CH_4: 3–10; O_2: 3–7	[170]
Poly(4-vinylpyridine)	He, H_2, N_2, O_2, CO_2, CH_4	158–162	35	3.3–10.5	[171]
Poly(ethylene-2,6-naphtalene dicarboxylate) (PEN)	H_2, CO_2	≈ 124 (Amorphous PEN)	20	2.96	[172]
Poly(oxyethylene)s with (alkylsulfonyl)methyl side chains	O_2	37–57	30	2.96[b]	[173]
Cardo poly(aryl ether ketone)s with pendent groups	H_2, N_2, O_2, CO_2, CH_4	239–266	25–100	5	[174]
Ladder polymer BBL and some semiladder polymers	He, N_2, O_2, CO_2, CH_4	NR	35–80	10	[175]
PIM-1, PIM-7 (Polymers of intrinsic porosity)	He, Ar, Xe, H_2, N_2, O_2, CO_2, CH_4	≥ 350	30	0.14–0.89	[176]

NR, not reported in cited reference; RH, relative humidity.
[a]Partial pressure difference.
[b]Pressure difference.

REFERENCES

1. R. M. Barrer, in *Permeability of Plastic Films and Coating to Gases, Vapors, and Liquids*, edited by H. P. Hopfenberg (Plenum Press, New York, 1974), p. 113.
2. W. R. Vieth, *Diffusion in and Through Polymers* (Hanser, Munich, 1991).
3. J. Crank, *The Mathematics of Diffusion* (Clarendon Press, Oxford, 1975).
4. S. A. Stern and H. L. Frisch, Annu. Rev. Mater. Sci. 11, 523 (1981).
5. H. L. Frisch and S. A. Stern, Crit. Rev. Solid State Mater. Sci. 11, 123 (1983).
6. W. J. Koros and R. T. Chern, in *Handbook of Separation Processes*, edited by R. W. Rousseau (Wiley-Interscience, New York, 1987), p. 862.
7. S. A. Stern and S. Trohalaki, in *Barrier Polymers and Structures*, edited by W. J. Koros, ACS Symposium Series No. 423 (American Chemical Society, Washington, DC, 1990), p. 22.
8. S. Kimura and T. Hirose, in *Polymers for Gas Separation*, edited by N. Toshma (VCH, New York, 1992), p. 15.
9. S. A. Stern, J. Membr. Sci. 94, 1 (1994).
10. R. M. Barrer, in *Diffusion in Polymers*, edited by J. Crank and G. S. Park (Academic Press, New York, 1968), p. 165.
11. G. S. Park, in *Diffusion in Polymers*, edited by J. Crank and G. S. Park (Academic Press, New York, 1968), p. 141.
12. V. Stannett, H. B. Hopfenberg, and J. H. Petropoulos, in *Macromolecular Science NTP International Review*, edited by C. E. H. Bawn (Butterworth, London, 1972), vol. 8, p. 329.
13. H. B. Hopfenberg and V. T. Stannett, in *The Physics of Glassy Polymers*, edited by R. N. Haward (Wiley, New York, 1973), p. 504.
14. J. H. Petropoulos and P. P. Roussis, in *Permeability of Plastic Films and Coatings to Gases, Vapors and Liquids*, edited by H. B. Hopfenberg (Plenum Press, New York, 1974), p. 219.
15. H. L. Frisch, J. Polym. Eng. 20, 2 (1980).
16. C. J. Durning, J. Polym. Sci., Polym. Phys. 23, 1831 (1985).
17. J. H. Petropoulos, in *Polymeric Gas Separation Membranes*, edited by D. R. Paul and Y. P. Yamkpol'skii (CRC Press, Boca Raton, 1994), p. 17.
18. C. A. Kumins and T. K. Kwei, in *Diffusion in Polymers*, edited by J. Crank and G. S. Park (Academic Press, New York, 1968), p. 108.
19. H. Sun, J. Phys. Chem. B 38, 7338 (1998).
20. H. Sun, P. Ren, and J. R. Fried, Comput. Theor. Polym. Sci. 8, 229 (1998).
21. A. S. Gusev, F. Müller-Plathe, and W. F. van Gunsteren, Adv. Polym. Sci. 116, 207 (1994).
22. F. Müller-Plathe, Acta Polym. 45, 259 (1994).
23. D. N. Theodorou, in *Diffusion in Polymers*, edited by P. Neogi (Marcel Dekker, Inc., New York, 1996).
24. J. R. Fried, in *Materials Science of Membranes for Gas and Vapor Separations*, edited by Y. Yampolskii, I. Pinnau, and B. D. Freeman (John Wiley & Sons, Ltd, West Sussex, UK, 2006), p. 93.
25. G. S. Heffelfinger and F. von Swol, J. Chem. Phys. 100, 7548 (1994).
26. A. Thompson and G. S. Heffelfinger, J. Chem. Phys. 110, 10693 (1999).
27. S. Pauly, in *Polymer Handbook*, edited by J. Brandrup and E. H. Immergut (Wiley-Interscience, New York, 1968), p. VI/435.
28. S. T. Hwang, C. K. Choi, and K. Kammermeyer, Sep. Sci. 9, 461 (1974).
29. V. T. Stannett, W. J. Koros, D. R. Paul, *et al*., Polym. Sci. 32, 69 (1979).
30. W. J. Koros, ed. *Barrier Polymers and Structures*. ACS Symposium Series. No. 423 (American Chemical Society, Washington, DC, 1990).
31. *Permeability Data for Aerospace Applications*, NAS1-388 (IIT Research Institute, Chicago, IL, March, 1968).
32. W. J. Koros, M. R. Coleman, and D. R. B. Walker, Annu. Rev. Mater. Sci. 22, 47 (1992).
33. W. J. Koros, G. K. Fleming, S. M. Jordan, *et al*., Prog. Polym. Sci. 13, 339 (1988).

34. R. R. Zolandz and G. K. Fleming, in *Membrane Handbook*, edited by W. S. W. Ho and K. K. Sirkar (Nostrand Reinhold, New York, 1992), p. 25.
35. M. Salame, in *The Wiley Encyclopedia of Packaging Technology*, edited by M. Bakker (Wiley, New York, 1986), p. 48.
36. G. S. Patil, M. Bora, and N. N. Dutta, J. Membr. Sci. 101, 145 (1995).
37. J. Y. Park and D. R. Paul, J. Membr. Sci. 125, 23 (1997).
38. L. M. Robeson, C. D. Smith, and M. Langsam, J. Membr. Sci. 132, 33 (1997).
39. Y. Yampol'skii, S. Shishatskii, A. Alientiev, *et al*., J. Membr. Sci. 148, 59 (1998).
40. Y. Yampol'skii, S. Shishatskii, A. Alientiev, *et al*., J. Membr. Sci. 149, 203 (1998).
41. A. Alentiev, K. A. Loza, and Y. P. Yampol'skii, J. Membr. Sci. 167, 91 (2000).
42. A. S. Michaels and A. J. Bixler, J. Polym. Sci. 50, 413 (1961).
43. S. A. Stern, S. R. Sampat, and S. S. Kulkarni, J. Polym. Sci., Part B: Polym. Phys. 24, 2149 (1986).
44. S. A. Stern, S. M. Fang, and R. M. Jobbins, J. Macromol. Sci. B5, 41 (1971).
45. A. W. Myers, C. E. Rogers, V. Stannett, *et al*., in *Proceedings of the 13th Annual Technical Conference, Society of Plastics Engineers*, St. Louis, Missouri, 1957.
46. Y. Naito, K. Mizoguchi, K. Terada, *et al*., J. Polym. Sci., Part B: Polym. Phys. 29, 457 (1991).
47. C. L. Kiplinger, D. F. Persico, R. J. Lagow, *et al*., J. Appl. Polym. Sci. 31, 2617 (1986).
48. G. J. van Amerongen, J. Appl. Phys. 17, 972 (1946).
49. J. Y. Lai and G. J. Wu, J. Appl. Polym. Sci. 34, 559 (1987).
50. A. K. Taraiya, G. A. Orchard, and I. M. Ward, J. Appl. Polym. Sci. 41, 1659 (1990).
51. K. Toi, Polym. Eng. Sci. 20, 30 (1980).
52. B. P. Tikhomorov, H. B. Hopfenberg, V. Stannett, *et al*., Makromol. Chem. 118, 177 (1968).
53. M. Salame, in *Proceedings of the Polymers, Laminations, and Coatings Conference*, Nashville, TN, 1986, p. 363.
54. M. Salame, in *Proceedings of the ACS 164th Meeting*, 1972, p. 113.
55. K. Toi, Y. Maeda, and T. Tokuda, J. Membr. Sci. 13, 15 (1983).
56. G. Morel and D. R. Paul, J. Membr. Sci. 10, 273 (1982).
57. J. A. Barrie and K. Munday, J. Membr. Sci. 13, 175 (1983).
58. H. Yasuda and K. Rosengren, J. Appl. Polym. Sci. 14, 2839 (1970).
59. A. W. Myers, V. Tammela, V. Stannett, *et al*., Mod. Plast. 37, 139 (1960).
60. J. M. Mohr and D. R. Paul, J. Appl. Polym. Sci. 42, 1711 (1991).
61. A. W. Myers, J. A. Meyer, C. E. Rogers, *et al*., TAPPI 44, 58 (1961).
62. N. Choji, W. Pusch, M. Satoh, *et al*., Desalination 53, 347 (1985).
63. R. Cowling and G. S. Park, J. Membr. Sci. 5, 199 (1979).
64. J. A. Barrie, P. Sagoo, and A. J. Thomas, J. Membr. Sci. 43, 229 (1989).
65. G. J. van Amerongen, J. Polym. Sci. 2, 381 (1987).
66. W. J. Koros and D. R. Paul, J. Polym. Sci., Polym. Phys. 16, 2171 (1978).
67. P. Mercea, T. Virag, and D. Silipas, Polym. Commun. 28, 31 (1987).
68. A. G. Wonders and D. R. Paul, J. Membr. Sci. 5, 63 (1979).
69. M. W. Hellums, W. J. Koros, G. R. Husk, *et al*., J. Membr. Sci. 46, 93 (1989).
70. T. A. Barbari, W. J. Koros, and D. R. Paul, J. Membr. Sci. 42, 69 (1989).
71. V. L. Simril and A. Hershberger, Mod. Plast. 27, 95 (1950).
72. S. A. Stern, S. K. Sen, and A. K. Rao, J. Macromol. Sci.—Phys. B10, 507 (1974).
73. A. C. Puleo, D. R. Paul, and S. S. Kelley, J. Membr. Sci. 47, 301 (1989).
74. A. Y. Houde and S. A. Stern, J. Membr. Sci. 92, 95 (1994).
75. Y. Wang and A. J. Easteal, J. Membr. Sci. 157, 53 (1999).
76. R. A. Pasternak, M. V. Christensen, and J. Heller, Macromolecules 3, 366 (1970).
77. N. Y. Yan, R. M. Felder, and W. J. Koros, J. Appl. Polym. Sci. 25, 1755 (1980).
78. R. A. Pasternak, G. L. Burns, and J. Heller, Macromolecules 4, 470 (1971).
79. R. M. Barrer and H. T. Choi, J. Polym. Sci., Part C: Polym. Symp. 10, 111 (1965).
80. S. A. Stern, V. M. Shah, and B. J. Hardy, J. Polym. Sci., Part B: Polym. Phys. 25, 1263 (1987).
81. C. Lee, H. L. Chapman, M. E. Cifuentes, *et al*., J. Membr. Sci. 38, 55 (1988).
82. S. A. Stern and B. D. Bhide, J. Appl. Polym. Sci. 38, 2131 (1989).
83. B. D. Bhide and S. A. Stern, J. Appl. Polym. Sci. 42, 2397 (1991).
84. S. M. Allen, M. Fuji, V. M. Stannett, *et al*., J. Membr. Sci. 2, 153 (1977).
85. G. S. Huvard, V. T. Stannett, W. J. Koros, *et al*., J. Membr. Sci. 6, 185 (1980).
86. V. T. Stannett, G. R. Ranade, and W. J. Koros, J. Membr. Sci. 10, 219 (1982).
87. R. Waack, N. H. Alex, H. L. Frisch, *et al*., Ind. Eng. Chem. 47, 2524 (1955).
88. W. Heilman, V. Tammela, J. A. Meyer, *et al*., Ind. Eng. Chem. 48, 821 (1956).
89. L.-T. Liu, I. J. Britt, and M. A. Tung, J. Appl. Polym. Sci. 71, 197 (1999).
90. W. W. Brandt, J. Polym. Sci. 41, 415 (1959).
91. R. Ash, R. M. Barrer, and D. G. Palmer, Polymer 11, 421 (1970).
92. A. Singh, K. Ghosal, B. D. Freeman, *et al*., Polymer 40, 5715 (1999).
93. H. Hachisuka, Y. Tsujita, A. Takizawa, *et al*., J. Polym. Sci., Part B: Polym. Phys. 29, 11 (1991).
94. K. J. Okamoto, K. Tanaka, and H. Kita, J. Polym. Sci., Part B: Polym. Phys. 27, 2621 (1989).
95. T. H. Kim, W. J. Koros, G. R. Husk, *et al*., J. Membr. Sci. 37, 45 (1988).
96. R. T. Chern, W. J. Koros, E. S. Sanders, *et al*., J. Membr. Sci. 15, 157 (1983).
97. S. A. Stern, Y. Mi, and H. Yamamoto, J. Polym. Sci., Part B: Polym. Phys. 27, 1887 (1989).
98. K. Okamoto, K. Tanaka, H. Kita, *et al*., Polym. J. 24, 451 (1992).
99. K. Okamoto, K. Tanaka, H. Kita, *et al*., J. Polym. Sci., Part B: Polym. Phys. 27, 1221 (1989).
100. K. Tanaka, H. Kita, K. Okamoto, *et al*., Polym. J. 21, 127 (1989).
101. K. Tanaka, H. Kita, K. Okamoto, *et al*., J. Membr. Sci. 47, 203 (1989).
102. K. Matsumoto and P. Xu, J. Membr. Sci. 81, 23 (1993).
103. K. Tanaka, M. Okano, H. Toshino, *et al*., J. Polym. Sci., Part B: Polym. Phys. 30, 907 (1992).
104. H. Yamamoto, Y. Mi, S. A. Stern, *et al*., J. Polym. Sci., Part B: Polym. Phys. 28, 2291 (1990).
105. C. Staudt-Bickel and W. J. Koros, J. Membr. Sci. 170, 205 (2000).
106. A. Shimazu, T. Miyazaki, M. Maeda, *et al*., J. Polym. Sci., Part B: Polym. Phys. 38, 2525 (2000).
107. A. Shimazu, T. Miyazaki, T. Matsushita, *et al*., J. Polym. Sci., Part B: Polym. Phys. 37, 2941 (1999).
108. G. Maier, M. Wolf, M. Bleha, *et al*., J. Membr. Sci. 143, 115 (1998).
109. S. L. Liu, M. L. Chng, T. S. Chung, *et al*., J. Polym. Sci., Part B: Polym. Phys. 42, 2769 (2004).
110. D. Ayala, A. E. Lozano, J. D. Abajo, *et al*., J. Membr. Sci. 215, 61 (2003).
111. J. Huang, R. J. Cranford, T. Matsuura, *et al*., J. Membr. Sci. 215, 129 (2003).
112. Y.-C. Wang, S.-H. Huang, C.-C. Hu, *et al*., J. Membr. Sci. 248, 15 (2005).
113. W.-H. Lin and T.-S. Chung, J. Membr. Sci. 186, 183 (2001).
114. A. Shimazu, T. Miyazaki, S. Katayama, *et al*., J. Polym. Sci., Part B: Polym. Phys. 41, 308 (2003).
115. J.-H. Kim, S.-B. Lee, and S. Y. Kim, J. Appl. Polym. Sci. 77, 2756 (2000).
116. R. Wang, S. S. Chan, Y. Liu, *et al*., J. Membr. Sci. 199, 191 (2002).
117. S. S. Chan, R. Wang, T.-S. Chung, *et al*., J. Membr. Sci. 210, 55 (2002).
118. T.-S. Chung, C. Cao, and R. Wang, J. Polym. Sci., Part B: Polym. Phys. 42, 354 (2004).
119. J. W. Xu, M. L. Chng, and T. S. Chung, Polymer 44, 4715 (2003).
120. L. Yang, J. Fang, and N. Meichin, Polymer 42, 2001 (2001).
121. J. Fang, H. Kita, and K.-i. Okamoto, J. Membr. Sci. 182, 245 (2001).
122. I. Kresse, A. Usenko, J. Springer, *et al*., J. Polym. Sci., Part B: Polym. Phys. 37, 2183 (1999).

123. J. Huang, R. J. Cranford, T. Matsuura, *et al*., J. Appl. Polym. Sci. 87, 2306 (2003).
124. Z.-K. Xu, M. Bohning, J. D. Schultze, *et al*., Polymer 38, 1573 (1997).
125. K. H. Hsieh, C. C. Tsai, and S. M. Tseng, J. Membr. Sci. 49, 341 (1990).
126. K. H. Hsieh, C. C. Tsai, and D. M. Chang, J. Membr. Sci. 56, 279 (1991).
127. L.-S. Teo, C.-Y. Chen, and J.-F. Kuo, J. Membr. Sci. 141, 91 (1998).
128. H. Liu and B. D. Freeman, J. Membr. Sci. 239, 105 (2004).
129. A. A. Lapkin, O. P. Roschupkina, and O. M. Ilinitch, J. Membr. Sci. 141, 223 (1998).
130. G. Perego, A. Roggero, R. Sisto, *et al*., J. Membr. Sci. 55, 325 (1991).
131. B. Kruczek and T. Matsuura, J. Membr. Sci. 146, 263 (1998).
132. R. T. Chern, F. R. Sheu, L. Jia, *et al*., J. Membr. Sci. 35, 103 (1987).
133. E. Sada, H. Kumazawa, P. Xu, *et al*., J. Appl. Polym. Sci. 38, 687 (1989).
134. C. L. Aitken, W. J. Koros, and D. R. Paul, Macromolecules 25, 3424 (1992).
135. A. J. Erb and D. R. Paul, J. Membr. Sci. 8, 11 (1981).
136. H. Kumazawa, J. S. Wang, and E. Sada, J. Polym. Sci., Part B: Polym. Phys. 31, 881 (1993).
137. W. Liu, T. Chen, and J. Xu, J. Membr. Sci. 53, 203 (1990).
138. Y. Dai, M. D. Guiver, G. P. Robertson, *et al*., Macromolecules 36, 6807 (2003).
139. K. J. Lee, J. Y. Jho, Y. S. Kang, *et al*., J. Membr. Sci. 212, 147 (2003).
140. K. J. Lee, J. Y. Jho, Y. S. Kang, *et al*., J. Membr. Sci. 223, 1 (2003).
141. I.-W. Kim, K. J. Lee, J. Y. Jho, *et al*., Macromolecules 34, 2908 (2001).
142. N. A. Platé, A. K. Bokarev, N. E. Kaliuzhnyi, *et al*., J. Membr. Sci. 60, 13 (1991).
143. Y. Ichiraku, S. A. Stern, and T. Nakagawa, J. Membr. Sci. 34, 5 (1987).
144. V. V. Teplyakov, D. Roizard, E. Favre, *et al*., J. Membr. Sci. 220, 165 (2003).
145. T. C. Merkel, V. Bondar, K. Nagai, *et al*., J. Polym. Sci., Part B: Polym. Phys. 38, 273 (2000).
146. S. V. Dixon-Garrett, K. Nagai, and B. D. Freeman, J. Polym. Sci., Part B: Polym. Phys. 38, 1078 (2000).
147. K. Nagai, L. G. Toy, B. D. Freeman, *et al*., J. Polym. Sci., Part B: Polym. Phys. 40, 2228 (2002).
148. K. Takada, H. Matsuya, T. Masuda, *et al*., J. Appl. Polym. Sci. 30, 1605 (1985).
149. M. Teraguchi and T. Masuda, Macromolecules 35, 1149 (2002).
150. T. Kanaya, I. Tsukishi, K. Kaji, *et al*., Macromolecules 35, 5559 (2002).
151. K. Nagai, L. G. Toy, B. D. Freeman, *et al*., J. Polym. Sci., Part B: Polym. Phys. 38, 1474 (2000).
152. K. E. Min and D. R. Paul, J. Polym. Sci., Part B: Polym. Phys. 26, 1021 (1988).
153. V. Stannett and J. L. Williams, J. Polym. Sci., Part C: Polym. Symp. 10, 45 (1965).
154. J. S. Chiou and D. R. Paul, J. Membr. Sci. 45, 167 (1989).
155. G. Maier, M. Wolf, M. Bleha, *et al*., J. Membr. Sci. 143, 105 (1998).
156. I. H. Musselman, L. Li, L. Washmon, *et al*., J. Membr. Sci. 152, 1 (1999).
157. K. Nagai, B. D. Freeman, A. Cannon, *et al*., J. Membr. Sci. 172, 167 (2000).
158. C. J. Orme, M. K. Harrup, T. A. Luther, *et al*., J. Membr. Sci. 186, 249 (2001).
159. H. J. Lehermeier, J. R. Dorgan, and J. D. Way, J. Membr. Sci. 190, 243 (2001).
160. A. J. Kelkar and D. R. Paul, J. Membr. Sci. 181, 199 (2001).
161. Z.-K. Xu, C. Dannenberg, J. Springer, *et al*., J. Membr. Sci. 205, 23 (2002).
162. C. Garcia, P. Tiemblo, A. E. Lozano, *et al*., J. Membr. Sci. 205, 73 (2002).
163. S. Kazama, T. Teramoto, and K. Haraya, J. Membr. Sci. 207, 91 (2002).
164. Z. Wang, T. Chen, and J. Xu, J. Appl. Polym. Sci. 83, 791 (2002).
165. J.-C. Lee, M. H. Litt, and C. E. Rogers, J. Polym. Sci., Part B: Polym. Phys. 36, 75 (1998).
166. Z. Y. Wang, P. R. Moulinie, and Y. P. Handa, J. Polym. Sci., Part B: Polym. Phys. 36, 425 (1998).
167. K. D. Dorkenoo, P. H. Pfromm, and M. E. Rezac, J. Polym. Sci., Part B: Polym. Phys. 36, 797 (1998).
168. E. S. Finkelshtein, M. L. Gringolts, N. V. Ushakov, *et al*., Polymer 44, 2843 (2003).
169. S. R. Thrasher and M. E. Rezac, Polymer 45, 2641 (2004).
170. C. M. Zimmerman and W. J. Koros, J. Polym. Sci., Part B: Polym. Phys. 37, 1235 (1999).
171. J.-J. Shieh and T. S. Chung, J. Polym. Sci., Part B: Polym. Phys. 37, 2851 (1999).
172. L. Hardy, E. Espuche, G. Seytre, *et al*., J. Appl. Polym. Sci. 89, 1849 (2003).
173. S.-Y. Kwak and J.-C. Lee, Macromolecules 33, 8466 (2000).
174. Z. Wang, T. Chen, and J. Xu, Macromolecules 33, 5672 (2000).
175. C. M. Zimmerman and W. J. Koros, Polymer 40, 5655 (1999).
176. P. M. Budd, K. J. Msayib, C. E. Tattershall, *et al*., J. Membr. Sci. 251, 263 (2005).